Efficacy of a multimolecular extraction from formalin-fixed paraffin-embedded tissue

A Thesis Presented to
The Faculty of Graduate Studies
of
Lakehead University
by
Nancy Cummings

In partial fulfillment of requirements
for the degree of
Master of Science in Biology

May 21, 2021

Declaration:

I hereby declare that this submission is my own work and that, to the best of my knowledge and belief, it contains no material previously published or written by another person, except where due acknowledgment has been made in the text.

All samples were donated postmortem and no animals were harmed for the purpose of this research. No ethics review was required as all samples were donated postmortem and were agricultural or hunting byproducts.

Nancy Cummings

Acknowledgements

I would like to acknowledge my graduate committee Dr. Michael Rennie and Dr. Wely Floriano for their support throughout my Masters project and for helping me to recognize when to scale back and when to push for more. A particular thanks to Dr. Rennie for advocating for me when Dr. Matheson left the country. I would also like to thank my committee members and external reviewer, Dr. Campbell for their time and consideration in reviewing my thesis. I would like to thank and acknowledge Dr. Carney Matheson for taking me on as a student and for always believing in my research capacity.

I would like to thank Ryan Lehto and the team at Global Genetic Health Inc. for allowing me access to their laboratory facilities and for providing technical support. As well as Stephen Fratpietro and the PaleoDNA lab for their assistance with testing and analysis.

A special acknowledgement to all the Matheson lab for being my support system, in particular Ashley Salamon, for her continual support and patience throughout the long nights in the lab and for making the masters process bearable. She was always there to make a bad day better.

Most importantly I would like to acknowledge the love, support, and sacrifices of my family without whom I would never have had the courage and strength to make it through. Thank you to my partner for making sure I remembered to eat and ensuring that I saw the sun on occasion. Most of all, thank you to Sydney who has been my guiding light and put up with mom's late nights and crazy deadlines.

Table of Contents

Acknowledgements ii
Table of Contents iii
List of Figures iv
List of Tables vi
List of Abbreviations vii
Abstract viii
Lay Summary ix
1.0 Introduction 1
2.0 Methods and Procedures 11
2.1 Sample Preparation and Experimental Procedures 12
2.2 Amplification and Sequencing 16
2.3 Data Analysis 17
3.0 Results 18
3.1 Sample Preparation and Experimental Procedures 18
3.2 Amplification and Sequencing 20
3.3 Data Analysis 21
4.0 Discussion 25
5.0 Conclusion 30
7.0 References 31
Appendix A 35
Appendix B 36
Appendix C 39
Appendix D 40
Appendix E 41
Appendix F 42
Appendix G 45
Appendix H 47
Appendix I 48

List of Figures

Figure 1. Methodological approach and work flow. 12

Appendix Figure 1.NCBI Blast search results for DNA Deer F1 GAPDH forward TRIzol® extracted. 48
Appendix Figure 2.Sequence alignment for DNA Deer F1 GAPDH forward TRIzol® extracted. 48
Appendix Figure 3. NCBI Blast search results for DNA Deer F1 GAPDH reverse TRIzol® extracted. 49
Appendix Figure 4. Sequence alignment for DNA Deer F1 GAPDH reverse TRIzol® extracted. 49
Appendix Figure 5. NCBI Blast search results for DNA Cow FFPE2 GAPDH forward TRIzol® extracted. 49
Appendix Figure 6. Sequence alignment for DNA Cow FFPE2 GAPDH forward TRIzol® extracted. 50
Appendix Figure 7. NCBI Blast search results for RNA Deer FF2 GAPDH forward TRIzol® extracted. 50
Appendix Figure 8. Sequence alignment for RNA Deer FF2 GAPDH forward TRIzol® extracted. 51
Appendix Figure 9. NCBI Blast search results for RNA Deer FF2 GAPDH reverse TRIzol® extracted. 51
Appendix Figure 10. Sequence alignment for RNA Deer FF2 GAPDH reverse TRIzol® extracted. 52
Appendix Figure 11. NCBI Blast search results for RNA Cow FFPE1 GAPDH forward TRIzol® extracted. 52
Appendix Figure 12. Sequence alignment 1 for RNA Cow FFPE1 GAPDH forward TRIzol® extracted. 52
Appendix Figure 13. Sequence alignment 2 for RNA Cow FFPE1 GAPDH forward TRIzol® extracted. 53

Appendix Figure 14. NCBI Blast search results for RNA Sheep F1 GAPDH forward GuSCN extracted. 53
Appendix Figure 15. Sequence alignment 2 for RNA Sheep F1 GAPDH forward GuSCN extracted. 53
Appendix Figure 16. NCBI Blast search results for RNA Sheep F1 GAPDH reverse GuSCN extracted. 54
Appendix Figure 17. Sequence alignment 2 for RNA Sheep F1 GAPDH reverse GuSCN extracted. 54

List of Tables

Table 1. Primer targets for qPCR amplification of cytokine and housekeeping genes for bovine, ovine, and odocoileus brain samples..... 17
Table 2. qPCR extraction results by preservation method..... 22
Table 3. RT-qPCR extraction results by preservation method. 22
Table 4. DNA qPCR Melt Curve by extraction method and target amplicon. 23
Table 5. RNA RT-qPCR melt curve by extraction method and target amplicon. 24
Table 6. Sanger sequencing and NCBI BLAST match..... 25

Appendix Table 1. qPCR Master Mix set up parameters 39
Appendix Table 2. qPCR running parameters 39
Appendix Table 3. RT-qPCR Master mix set up parameters 40
Appendix Table 4. RT-qPCR running parameters..... 40
Appendix Table 5. DNA qPCR raw data..... 42
Appendix Table 6. RNA RT-qPCR raw data..... 45
Appendix Table 7. qPCR DNA samples sent for Sanger sequencing. 47
Appendix Table 8. RT-qPCR RNA samples sent for Sanger sequencing. 47

List of Abbreviations

ABI	Applied Biosystems
β2M	beta-2-microglobulin
β-ME	beta-mercaptoethanol
BLAST	basic local alignment search tool
bp	base pair
cDNA	complementary DNA
Ct	cycle threshold
ddNTP	dideoxynucleotide
DEPC	diethyl pyrocarbonate
dNTP	deoxynucleotide triphosphate
DTT	dithiothreitol
dsDNA	double stranded DNA
EDTA	Ethylenediaminetetraacetic acid
FF	formalin fixed
FFPE	formalin-fixed paraffin-embedded
GAPDH	Glyceraldehyde 3-phosphate dehydrogenase
GuSCN	guanidinium thiocyanate
HTS	high throughput sequencing
NaCl	sodium chloride
NCBI	National Center for Biotechnology Information
PCR	polymerase chain reaction
qPCR	quantitative polymerase chain reaction
ROX	carboxy-X-rhodamine
RNA	ribonucleic acid
RT-qPCR	reverse transcriptase quantitative polymerase chain reaction
SDS	sodium dodecyl sulfate
Taq	*Thermus aquaticus*
TE	tris-ethylenediaminetetraacetic acid
Tm	melting temperature
UV	ultraviolet

Abstract

As the genetic basis and gene expression components are being discovered for an increasing number of diseases and disorders there is a rising interest in using multiomic approaches to better understand these conditions. The large tissue banks of formalin fixed (FF) and formalin-fixed paraffin-embedded (FFPE) tissues present a unique opportunity to study rare conditions and difficult to sample organs such as brains. Current molecular studies on FFPE look at single molecule extractions, which provide only a partial picture of disease mechanisms. This study compared the efficacy of TRIzol®, a tri-molecule extraction method, to that of the traditional single molecule methods for DNA and RNA extraction in frozen, FF, and FFPE brain tissue using animal models. Optimization of this would allow for DNA and RNA to be obtained from the same sample providing a more accurate and comprehensive picture of the mechanism of disease or disorder. The quantity and purity of the DNA and RNA extracted from frozen, FF, and FFPE brain samples (aged for 3 years) were determined by spectrophotometry. Quality was determined by real-time PCR (qPCR) and reverse transcriptase qPCR (RT-qPCR) using beta-2-microglobulin (98bp) and glyceraldehyde 3-phosphate dehydrogenase (227bp) targets. Our study found no significant difference in efficacy between TRIzol® and the traditional methods employed in the literature, indicating that TRIzol® is comparable to the currently used, single molecule extractions when applied to FF and FFPE brain tissue. This finding requires further investigation with a larger set of samples, but if supported may help maximize the amount of information obtained from rare samples as multiple data sets would be obtained from a single sample. Unexpectedly, this study also observed a higher rate of success in extracting high quality RNA compared to DNA regardless of extraction method. Due to the low number of samples, the statistical significance of this observation could not be established however we feel that it warrants further investigation.

Lay Summary

Genetics and gene expression have become increasingly important in disease research, but it can often be difficult to acquire adequate samples if the medical condition is very rare or if the condition affects a part of the central nervous system, such as the brain. This problem can be mitigated if archived biomedical samples such as formalin-fixed paraffin-embedded tissue blocks taken during surgery and autopsy can be used in biomolecular research. Extraction of DNA and RNA from these samples has two main problems. First, the preservation method used makes it difficult to extract high quality DNA and RNA. Secondly, because DNA or RNA extraction is a destructive process and these samples are often small, frequently only one of these can be obtained from a sample using traditional methods. This study assessed the ability of TRIzol®, a multimolecular extraction reagent, to extract both DNA and RNA simultaneously from a tissue block sample. We demonstrated that there was no significant difference between the extraction methods in the amount or quality of DNA and RNA obtained. Using TRIzol® to simultaneously extract DNA and RNA will allow researchers to generate multiple sets of information from a single sample and enable a greater number of studies to be conducted while reducing the number of samples needed.

1.0 Introduction

One of the major barriers to studying rare diseases and diseases affecting difficult to sample tissues is the availability of samples from living or recently deceased donors. This barrier can be reduced if archived tissues can be made feasible for molecular analysis. Tissues banks around the world contain thousands of archived histological samples and preserved specimens from necropsies and biopsies making them a potentially valuable source of research material.

Traditionally, histology has been used to diagnose disease and study tissues. While histology is still often used for this purpose, molecular approaches have begun to provide deeper insight into diseases, genetic disorders and pathologies with a genetic basis. Archived tissues, medical, veterinary, and archaeological, present a unique opportunity to not only study rare disorders but to study their presence and evolution throughout history. Unfortunately, preserved tissue often presents a unique set of challenges to obtaining quality molecular information.

Historically one of the largest challenges to the study of anatomy and disease was tissue preservation. Cadavers were dissected quickly, and paintings were used to preserve the information before the tissues decayed. Until the late 1800s, alcohol was used as a tissue fixative for histological samples and medical specimens, however ethanol preservation caused desiccation and cellular distortion, and alcohol quality was not consistent. While formaldehyde was first reported by Alexander Mikhailovich Butlerov in 1859 and formally identified in 1868 by August Wilhelm von Hofmann, its usefulness as a histological tissue preservative was first published 26 years later by Ferdinand Blum in 1894 (Fox, et. al., 1985). Formalin, the diluted form of formaldehyde, prevented the desiccation of samples that plagued alcohol-based fixation techniques. Formalin fixation combined with paraffin embedding (FFPE) allowed for minimal structural distortion and more accurate histological analysis of tissues (Titford, 2006). While immunohistochemistry remains a widely used diagnostic tool and tissue biopsies are routinely preserved as FFPE blocks, medical research has steadily moved towards a molecular understanding of disease and disorders. The advent of modern refrigeration made freezing tissue samples possible, enabling preservation of

molecular level information. Diagnostic methodologies, however, were developed on formalin fixed (FF) tissue and there is both a high real estate and maintenance cost involved with storing frozen tissue. For these reasons, FF and FFPE preservation are still the most commonly used methods. These vast libraries of preserved tissue samples provide an opportunity for molecular-based studies using large sample sizes which would be difficult to acquire otherwise. This is especially true in the case of molecular based studies involving rare diseases and difficult to sample tissues such as brain and spinal tissue.

One of the major barriers to using FF and FFPE tissues for molecular analysis is the damage that occurs during the preservation process. These types of preservation are useful for observing cell structure and cell abnormalities, but the formalin fixation process used in both of these preservation methods causes complications for molecular analysis including crosslinking, strand breaks, abasic sites, deamination of cytosine, and inhibition of deoxyribonucleic acid (DNA), ribonucleic acid (RNA), and protein analysis (Do & Dobrovic, 2015; Srinivasan, et. al., 2002). Additionally, these complications have been shown to increase with the duration of storage (Funabashi, et. al., 2012; Robbe, et. al., 2018). The time between death and sample fixation can also be a source of molecular degradation. While DNA is relatively resilient, seeming not to be significanlty damaged for up to 24 hours after death or excision, damage to RNA can begin quite quickly (Coombs, et. al., 1999; Do & Dobrovic, 2015). Most tissue bank samples have been collected during surgeries, autopsies, or necropsies, and the delay before fixation as well as the duration of fixation time can vary resulting in enzymatic breakdown or poor fixation (Kim, et. al., 2017; Do & Dobrovic, 2015). In addition, the wax used in FFPE preservation can cause chemical inhibition during extraction and can cause inhibition and equipment damage during downstream analysis if not completely removed during deparaffinization.

The efficacy of several methods of deparaffinization have been studied though there is little concensus on which method is best. The two methods most commonly applied in research are xylene deparaffinization with gradated ethanol washes to rehydrate and the application of heat to melt off the wax as well as help to break formalin induced crosslinking (Shi, et. al., 2004; Fraser, et. al., 2020). Residual xylene can cause inhibition in downstream analysis and may cause inaccurate ultraviolet (UV) absorption readings during quantificaiton (Khan, et.

al., 2018). On the other hand, the longer heating required for complete deparaffinization can introduce damage to nucleic acids and denature proteins, requiring additional sample if proteomic analysis is to be undertaken (Fabre, et. al., 2014). While both methods have been extensively employed the results have not consistently been replicated.

Despite the challenges involved, most of these types of damage can be accounted for during extraction and data analysis, and should not prevent FFPE from being used in molecular research, as long as protocols are optimized to account for these challenges (Spencer, et. al., 2013; Robbe, et. al., 2018; Esteve-Codina, et. al., 2017). The potential use in retroactive studies across many disciplines makes optimization of molecular methods for FFPE and FF tissue an important area of study.

Genetic components are being discovered for an increasing number of diseases and disorders, beginning with Huntington's disease being genetically mapped in 1983 (Gusella, et. al., 1983). Early genetic studies looked at human diseases with predominantly simple inheritance, but as technology has improved, more genetically complex diseases and disorders have been studied and across many species (Claussnitzer, et. al., 2020; Castelhano, et. al., 2009). Being able to effectively extract, purify, and analyze DNA is the foundation of modern genetic studies.

Many methods of DNA isolation have been developed but one of the most common methods when working with animal cells is a proteinase K digest coupled with a silica based purification. Proteinase K is a serine protease which hydrolyzes proteins at the peptide bond adjacent to the carboxylic acid group of aliphatic and aromatic amino acids (Ebeling, et. al., 1974). This broad spectrum of attack not only allows proteinase K to digest cellular surface proteins but also to degrade nucleases which would otherwise damage the DNA. Sodium dodecyl sulfate (SDS), a strong anionic detergent, is often added to increase the effectiveness of proteinase K and solubilize cell membranes. It does this by denaturing proteins thus making the sites of cleavage more accessible to the protease and disrupting the cell membrane (Hilz, et. al., 1975). This sudden release of the cell contents must be buffered near biological pH to prevent damage to the DNA. Trisaminomethane (Tris) is an effective buffer between pH 7-9 and is often used in cell lysis for this reason. Sodium chloride (NaCl) is

often added to the buffer to maintain an isotonic environment as well as prevent non-specific protein aggregation. Additives such as dithiothreitol (DTT) are used to disrupt disulfide bonds between proteins and scavenge nitrogen and oxygen radicals, protecting DNA from damage (Sölen, et. al., 1990), while ethylenediaminetetraacetic acid (EDTA) is added to chelate metal ions, deactivating cofactor dependent enzymes such as DNases and RNases (Chen, et. al., 1999).

Once the DNA has been extracted from the nucleus, it must be isolated and purified to allow downstream analysis. Silica based purification is commonly used across may fields and acts by adsorbing the DNA to acidified silica in the presence of a highly concentrated chaotropic salt (Boom, et. al., 1990). The high concentration of chaotropic salt, in this case 4M guanidinium thiocyanate (GuSCN), provides an excess of positive ions which form salt bridges between the negative backbone of the DNA and the negatively charged silica. It also serves to denature proteins making them more soluble by reducing hydrophobicity. This allows the remaining cellular components and salts to be washed away using ethanol and buffers, before eluting the DNA in water or a low salt, high pH buffer such as a tris-EDTA (TE) buffer (Boom, et. al., 1990). Low concentration buffers such as TE^{-4} are often used as the EDTA chelates any remaining divalent cations preventing DNase activity, and the tris buffer keeps the solution with a slightly basic pH (~8.0) which has been shown to protect DNA from hydrolytic damage without inhibiting downstream analysis (Kim, et. al., 2011).

As the role of DNA has become better understood, so too have the importance and varied roles of RNA. Once thought to be involved only in translation of DNA to proteins it has been found that RNA serves many roles beyond messenger, transport, and ribosomal RNA including gene regulation and epigenetic modifications (Morris, 2011; Gebert & MacRae, 2019). This is particularly important as the transcriptome, all the RNA within a cell, differs from organ to organ and even cell to cell as well as at different points in time. However, because RNA is a largely transient molecule, which is generally broken down quickly after translation, it can be more difficult to isolate than DNA. Currently, most transcriptomic work is carried out on fresh samples or samples which have been flash frozen and stored at -80°C to inhibit nuclease activity and RNA degradation. This can be largely impractical as -80°C freezers are expensive and not always standard laboratory equipment. In addition, care must

be taken when freezing to avoid as many freeze thaw cycles as possible as these have been shown to cause degradation (Wang, et. al., 2015).

One of the issues which must be overcome when isolating RNA is its separation from the DNA, as they are biochemically similar. An acid guanidinium thiocyanate phenol-chloroform extraction is commonly used as it takes advantage of the different solubilities of RNA and DNA using a phase separation (Chomczynski & Sacchi, 1987). An extraction solution containing guanidinium thiocyanate and sodium lauroyl sarcosinate (sarkosyl), a cold-tolerant anionic detergent, is used to denature the proteins and disrupt the cell membrane. A strong reducing agent such as beta-mercaptoethanol (β-ME) is commonly added to ensure that the RNases are completely denatured. Phenol, an organic solvent, is added to solubilize the lipids and denatured proteins. Because phenol is not miscible with the aqueous extraction solution an organic phase is formed. Excess hydrogen ions (H+) in the acidic aqueous environment, ~pH4, neutralize the phosphodiester bonds on the DNA backbone. This changes the total charge, of the DNA, to neutral rending it insoluble in the aqueous phase and forcing it into the organic phase. The single stranded nature of RNA leaves its bases unpaired and provides more sites of interaction with the H+ ions keeping the RNA in the aqueous phase due to its higher proteinase KA (Chomczynski & Sacchi, 1987). Isoamyl alcohol is used as an anti-foaming agent allowing the interface to remain sharp and chloroform is added to increase the separation between the two phases as phenol will retain 10-15% water and cause loss of RNA (Chomcyzynski & Sacchi, 2006). Isopropanol is used to precipitate the RNA from the upper aqueous phase. If the sample purity is insufficient for downstream analysis, an additional purification method such as ethanol precipitation is often employed. Sodium acetate provides positive ions precipitating RNA in the presence of 70% ethanol, while most contaminants remain in solution.

To gain a complete understanding of development, disease, disorder, and health, it is not enough to study the genetics or transcriptomics of an organism in isolation, as each provides only a partial picture. Multiomics refers to the study of multiple sets of information at once, allowing one to inform the other. This is particularly important when trying to understand the effect of environment on disease. Genomics informs which genes are present but cannot differentiate between which genes are being transcribed and which are inactive. The

transcriptome informs on gene regulation, expression, and the effects of environment but cannot identify the presence of genes which are not active. The transcriptome also varies from organism to organism, organ to organ and even cell to cell. Because of this variation, to obtain the most accurate set of information, the genome and transcriptome must be obtained from the same sample if possible.

Multimolecular extractions allow for the isolation of multiple sets of information from a single sample. This allows for a snapshot of the total RNA and DNA in a single section of tissues. TRIzol® is a proprietary optimized extraction reagent available from Invitrogen that uses similar phase separation chemistry to an RNA acid-guanidinium thiocyanate phenol-chloroform extraction (Chomczynski, 1993). While the chemistries appear to be similar, because TRIzol® is proprietary, the exact composition is unknown making them difficult to compare. One observable difference is the presence of an inert organic colourant which allows for a strong visual separation between phases. The TRIzol® method also uses fewer reagents, resulting in less handling of harmful chemicals during reagent preparation. Additionally, extraction of DNA and RNA using TRIzol® is less time consuming than either the proteinase K or acid-guanidinium thiocyanate phenol-chloroform method.

Ultraviolet (UV) absorbance spectrophotometry is often used to determine the efficacy of nucleic acid isolation and determine sample purity after extraction. This method of quantification and purity assessment is dependent on the specific absorbance spectra of DNA, RNA, proteins, and common contaminants. The aromatic rings of nucleic acid bases absorb UV light in the ~260nm range while proteins absorb at ~280nm. By taking the ratio of these two measurements, the purity of an extract can be estimated with an A_{260}/A_{280} ratio of 1.8 indicative of pure DNA and an A_{260}/A_{280} ratio of 2.0 for pure RNA (Doshii, et. al., 2009). By applying Beer-Lambert's law, $A=\varepsilon lc$, where A is absorbance, ε is the molar absorbance coefficient, l is the path length, and c is the concentration, the absorbance can be correlated with the concentration in absorbance units. This is then multiplied by the corresponding nucleic acid absorbance unit equivalent; 50μg/ml for DNA and 40μg/ml for RNA, to estimate the concentration (Doshii, et. al. 2009). Frequently, absorption is also measured at 320nm to identify particulate contamination, and 230nm to identify the presences of residual salts such as thiocyanates (Tsanev & Markov, 1960). Quantity is determined by applying

Beer-Lambert's Law to estimate the number of absorption units present. Specialized equipment such as the Nanodrop 2000c spectrophotometer have been developed to use microvolumes of sample to take these measurements and plot the absorbance curve based on the molecule selected. Where previous cuvette-based spectrophotometry required milliliters of sample these microvolume spectrophotometers require 1-2 microliters, making them more practical (Desjardins & Conklin, 2010). Determination of sample purity and quantity is highly important prior to downstream analysis, such as the polymerase chain reaction (PCR), as these often have volume requirements, and the presence of contaminants can inhibit reactions or confound results.

Since its discovery, PCR has revolutionized the field of nucleic acid research. By using well-designed, paired oligonucleotide primers and cycles of varying temperatures to initiate denaturation, annealing, and extension of the DNA, the PCR enables the DNA polymerase enzyme to copy a targeted sequence of DNA (Saiki, et. al., 1985). DNA polymerases can only add deoxynucleotides (dNTPs) onto an existing double strand of DNA. To facilitate targeted amplification, small single stranded oligonucleotide sequences, called primers, are included in the reaction. These bind to the ends of the target region of denatured DNA during the annealing phase of PCR, providing a small double stranded region for the polymerase to begin copying from. One primer for each strand is used, one forward and one reverse (Saiki, et. al., 1988). To ensure adequately tight binding and high affinity primers; they should be designed to be 40-60% cytosine (C) and guanine (G), have a G/C tail on the 3' end, have a melting temperature between 65-75°C, and have melting temperatures within 5°C of each other. Designing primers which are specific to the target and meet these criteria ensures that only the desired section of DNA is amplified. The denaturation stage of PCR heats the DNA to 94-98°C, which breaks the bonds holding the two strands together, thus denaturing the DNA. Once this is completed, the reaction is cooled to approximately 5°C below the melting temperature (T_m) of the lowest primer allowing the primers to anneal to their complimentary sequence of DNA (Rychlik, et. al., 1990). The temperature is then raised to 72°C, the temperature for optimal activity of the DNA polymerase. During the extension phase, the polymerase extends the primers in opposing directions creating two new fragments of DNA for the primers to anneal to and be copied during the next cycle, thus creating an exponential

rate of copying until the saturation of copied fragments is such that it inhibits access to available primers and dNTPs. Exponential copying of a specific section of DNA reduces sample requirements as the region of interest can be isolated using region specific primers and its concentration increased within the sample extract. This increased concentration allows for targeted sequencing of a specific region which had previously been impossible using Sanger sequencing.

The discovery of the *Thermus aquaticus* (*Taq*) bacteria and the isolation of its heat-resistant DNA polymerase enzyme allowed for the automation of PCR amplification. The heat tolerance of the *Taq* polymerase enzyme prevents the heat required to separate the strands of DNA from denaturing it. This means that new polymerase did not need to be added after each denaturation cycle (Saiki, et. al., 1988). The ability to automate this process has allowed PCR to be widely applied across many areas of research including medical and veterinary medicine. Just as PCR has been applied across many fields, new variations of PCR have been developed to fit these many applications.

Real-time or quantitative PCR (qPCR) is one of the most widely applied variations of PCR. This method is used to evaluate quality of extracted DNA, fidelity of amplification primers, and when applied to RNA research, it is used to determine expression levels. Using either fluorescent probes or an intercalating dye, such as SYBR green, qPCR uses spectrophotometric detection to determine the initial concentration, the rate of amplification during PCR, and can be used to plot a melt curve after the PCR is complete to ensure the specificity of the primers and a lack of primer dimers (Higuchi et. al., 1992). Because intercalating dyes only fluoresce when bound between double stranded DNA it is possible to determine the melting point of a qPCR product. To do this the qPCR product is slowly heated while the fluorescence is continuously measured. The point at which the dye signal is no longer detected indicates the temperature at which the strands have become completely separated, also known as the melting temperature (T_m). This can then be compared to the theoretical Tm of the target amplicon to infer the specificity of the amplification. The theoretical melting temperature is based on the amount of energy required to break the hydrogen bonds between the 2 strands of DNA. Because the expected sequence of the amplicon is known the exact theoretical melting temperature can be calculated and compared

to the actual melting temperature of the qPCR product (Higuchi et. al., 1992). While not definitive a melt curve is a good indicator of both quality and specificity of the qPCR product.

The identification of reverse transcriptase by Baltimore et al, (1970) further allowed PCR to be applied not only to DNA but also to RNA creating reverse transcription PCR (RT-PCR). To do this, reverse transcriptase is first used to reverse-transcribe RNA to complementary DNA (cDNA) and then the cDNA is used in PCR to amplify the target sequence. Coupling RT-PCR with qPCR (RT-qPCR) enables the study of gene expression in a particular sample at a particular time, as well as providing insight into post transcription editing. Gel electrophoresis is commonly used to confirm the accuracy of the amplification as well as ensure specificity and efficiency of the primers.

The development of Sanger sequencing in 1977 opened up the field of genetics by enabling the code of DNA to be read and eventually mapped to specific chromosomes (Sanger, et. al., 1977). Modern sanger sequencing uses a single primer PCR, for single direction copying, and a mixture of dNTPs and fluorescently-labelled dideoxynucleotides (ddNTPs) which are provided as building blocks to be used by the DNA polymerase for the creation of a complementary strand. The ddNTPs are incorporated at random and, as they lack the 3'-OH group with which to attach the next nucleotide, the strand is terminated (Sanger, et. al., 1977). These terminations generate strands of DNA of random size, with fluorescently labelled terminal bases. Repeating this process many times via PCR generates thousands of copies allowing the entire sequence to be determined. High throughput sequencing (HTS) technology has simplified the process and made it much less time consuming by using multi-use parallel capillary columns, instead of single use slab-gels, to increase the number of samples that can be read at a time and reducing the resources required to read them. With the application of an electrical current, the strands migrate through the capillaries by size with the smallest migrating through most quickly. As they mov through the capillary they pass through the detection window and the fluorescently labelled ddNTP at the terminal end is excited by a laser. The excited label emits light, the colour of which corresponds to the incorporated ddNTP. This light is recorded by a camera, allowing the sequence to be captured (Churko, et. al., 2013).

Sequence data are generated as electropherograms, which are then analyzed for accuracy and quality of data, both visually and using an analysis program such as SnapGene, which is designed to read electropherograms and allow data clean up. SnapGene, and similar programs, can also be used to compare the generated sequence to that of a known reference sample to identify sequence variations such as mutations.

Cleaned up sequences can also be compared to a sequence database such as the one at the National Center for Biotechnology Information (NCBI) using tools such as NCBI's Basic Local Alignment Search Tool (BLAST) for nucleotide sequences (Altschul, et. al., 1990). This tool compares the sequence from the sample to all those within the database and provides the statistical significance of the similarity between them. This data is often used to identify species and region on the chromosome which can be used to confirm the accuracy of a PCR amplification or identify an unknown sample.

The study of central nervous system samples, particularly brain samples, pose several challenges. There are the obvious concerns involved with obtaining fresh samples from humans and there are several physiological concerns with using laboratory animals. Unless great care is taken to prevent or mitigate their effects, unintentional introduction of stressors can change RNA and protein expression levels within the brain (Soverchia, et. al., 2005). While archived samples are in greater abundance and do not pose the same sorts of ethical concerns, they are often not representative of a healthy population, and the greater the time interval between death and fixation, the greater the potential for molecular degradation (Cummings et. al., 2001). Despite these challenges, the use of archived tissue in neuromolecular research continues to grow, but more research is needed to optimize the use of them.

Beyond the challenges with sample acquisiton, brain tissue itself poses several challenges. Brain tissue has a much higher fat content than other organs (O'Brien & Sampson, 1965). This can pose a challenge during molecular analysis and must be taken into account when designing a study. Brain tissue also tends to have a lower nucleic acid yield due to the high lipid content (Wang, et. al., 2013). The brain is also a physiologically complex organ, with high gene expression variation between regions (Sandberg, et. al., 2000). This poses a

difficult challenge as the distinction between regions is not easily determined, which means that extracting as much information as possible from a single sample may be the most accurate method of analysis (Soverchia, et. al., 2005; Sandberg, et. al., 2000).

This study evaluated the efficacy of using a multimolecular extraction reagent, TRIzol®, to extract high quality DNA and RNA from archived brain tissue and compare this to the efficacy of the more commonly employed single molecule extraction method for each, as found in the literature. This evaluation was done to determine the viability of applying this multimolecular extraction method to multiomic research where the amount of available sample is limited. To be considered a viable option it was determined that TRIzol® must be shown to be at least as effective if not more effective than the traditional extraction methods. The minimum standard of efficacy was determined to be no statistical difference between the rate of success of TRIzol® and any one traditional method. Success was defined as the ability to extract and isolate DNA or RNA of high enough quality to be successfully amplified.

2.0 Methods and Procedures

This study followed the same methodological approach for all samples and tissue preservation type, with the only variation being the extraction method applied (Figure 1). Duplicates of each species and preservation types were used. The only other variation was the type of qPCR employed, which was based on which nucleic acid was being amplified. Prior to extraction the FFPE samples were deparaffinized as described in Section 2.1.

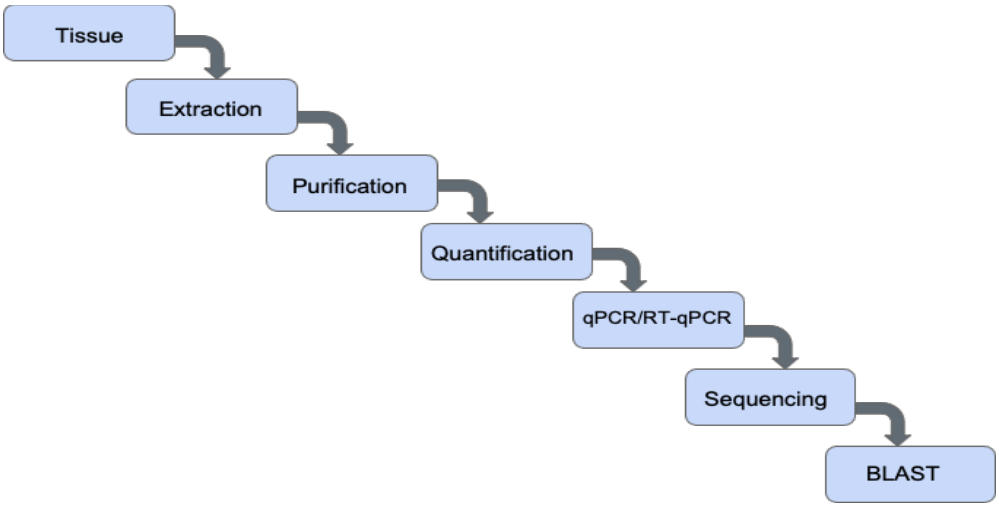

Figure 1. Methodological approach and work flow.
Work flow for samples beginning with tissue preparation for each sample type. FFPE samples have an additional deparaffinization step between Tissue and Extraction as described in Section 2.1.

2.1 Sample Preparation and Experimental Procedures

Sample Collection

Animal brains were harvested from three different species: cow (*Bos taurus*); white tailed deer (*Odocoileus virginianus*); and sheep (*Ovis aries*), within 12 hours of death and stored at -20°C until preservation could be performed. Brains were defrosted and placed into sterile plastic petri dishes. Using disposable scalpels and sterile tweezers, two 2x3cm pieces were sliced from each brain and placed into sterile 50mL conical tubes. Remaining brain samples were stored at -20°C.

A positive control was obtained using buccal swabs from the technician performing the benchwork. For each extraction method one buccal swab was rubbed on the inside of the cheek for 45 seconds to collect cheek cells. Each swab was done on a different part of the cheek to ensure maximum cell collection.

Frozen sample preparation

Using disposable scalpels and sterile tweezers, a $1mm^3$ cube piece of tissue from each type of brain sample was placed into sterile 2mL microcentrifuge tubes and stored at -20°C until digestion.

Formalin Fixation

To mimic formalin fixed (FF) archived tissue, brain sections were thawed. Using disposable scalpels two 2x3cm pieces were cut from each brain and placed into sterile 15mL tubes. Remaining brain samples were stored at -20°C. A volume of 20mL of cold 10% formalin was added to each sample. Samples were incubated for 12 hours at room temperature (21°C) prior to decanting off the formalin solution. A second volume of 10mL of fresh 10% formalin was added to each, and then incubated at room temperature for 12 hours. The formalin solution was decanted, and the same volume of fresh formalin (10mL) was added a third time, and incubation continued for an additional 24 hours, for a total fixation time of 48 hours. All samples were then stored at room temperature out of direct light for 3 years to simulate archived sample storage conditions.

Formalin-Fixation Paraffin-Embedding

To mimic formalin-fixed, paraffin-embedded (FFPE) archived tissue samples two portions of each the brains samples were formalin fixed and paraffin embedded by following a modified IHC World protocol (Appendix A) (IHC World). To fix the tissue, 20mL of 10% formalin was added to each conical tube and the samples were incubated at room temperature for 24 hours. The formalin solution was then decanted off. A second volume of 20mL of 10% formalin was added to the remaining samples, and then incubated for an additional 24 hours prior to decanting the formalin. To dehydrate the samples, they were soaked, at room temperature, in increasing concentrations of ethanol for the following lengths of time; 70% ethanol for 1 hour twice, then 80% ethanol for 1 hour, 95% ethanol for 1 hour, followed by 100% ethanol for 1.5 hours. Samples were then soaked in 15mL of xylene three times for 1.5 hours each time. A volume of 10mL of melted paraffin was added to each tube, and samples were incubated at 59°C in a water bath for 2 hours. Wax was then decanted. A second volume of 15mL of melted paraffin was added to each tube and samples were incubated at 59°C in a water bath for 2 hours. Wax was then decanted and discarded.

Deparaffinization

Prior to extraction, two replicates of FFPE tissue from each sample type were deparaffinized. Using disposable scalpels and sterile tweezers, a $1mm^3$ cube of each tissue was cut from the 2x3cm block and placed into sterile microcentrifuge tubes. Deparaffinization of each was carried out according to the method outlined in Standard Protocols for Formalin-Fixed Paraffin-Embedded Tissues (Appendix A)(IHC World) using the method for samples more than 25μm thick.

Proteinase K Extraction

Samples were aliquoted in 1mm punches into sterile 2mL microcentrifuge tubes, extraction buffer was added to each sample as well as a reaction negative control, which contained no tissue sample, for final concentrations of 7.2mM Tris-HCl; 72.2mM NaCl; 0.72mM EDTA; 34.7mM DTT; 2.2% w/v SDS. Frozen samples and the reagent negative were digested with 10μL of 20mg/mL proteinase K and 25μL of sterile water (ddH_2O), while FF and FFPE samples were digested with 30μL of proteinase K. The total volume of each reaction was 450μL. The FFPE samples were pretreated by heating to 75°C in 1.5mL of ddH_2O, for 30 minutes to melt any remaining paraffin, then cooled at 4°C. Once cooled, paraffin was scraped off the top of the water, the sample was rinsed with ddH_2O and then removed to new sterile 2mL microcentrifuge tube. All samples were ground with sterile disposable pestles for 45 seconds to homogenize prior to extraction buffer being added. All samples were vortexed for 30 seconds to ensure homogenization, then incubated at 56°C for 24 hours with 450rpm agitation before purification by silica bead purification (Boom, et. al., 1990), as described below.

Acid Guanidinium Thiocyanate-Phenol-Chloroform extraction

Samples were aliquoted in 1mm punches into 2mL microcentrifuge tubes. Prior to extraction each sample was ground for 45 seconds with a sterile disposable pestle to ensure homogenization. The extractions of RNA were performed using the methods outlined in Chomcyznski and Sacchi (2006). Purification was performed by ethanol precipitation prior to quantification (Rio, et. al., 2010).

TRIzol® Extraction

To compare the standard single molecule extraction methods with the efficiency of a multimolecular extraction method, TRIzol® was chosen as this method allows for the simultaneous isolation of DNA, RNA, and proteins using the differential solubilities of each component. As this study focuses on the efficiency of DNA and RNA extraction from a single sample TRIzol® extractions were performed as per manufacturer instructions to obtain DNA and RNA from a single sample using the suggested modifications for tissues with a high lipid content (Appendix B)(Invitrogen, 2016). The protein layer was stored at -80ºC for future analysis.

Sample Purification

The proteinase K extracted DNA samples were purified using a modified silica bead purification, with two working wash buffer washes and a 75% ethanol wash to remove organic contaminants (Boom, et. al., 1990). The DNA samples were resuspended in 100µL TE^{-4} buffer and incubated at 56ºC for 1 hour to release DNA from silica beads. After incubation, samples were centrifuged for 30 seconds at 13,000rpm and the supernatant transferred to a new sterile microcentrifuge tube.

All TRIzol® extracted DNA and RNA samples as well as the acid-guanidinium phenol-chloroform extracted RNA samples were purified using an ethanol precipitation in addition to the purification included in the original protocols (Chomcyzynski & Sacchi, 2006). For ethanol precipitation, a 10% volume (10µL) of 3M sodium acetate was added to the total volume of resuspended nucleic acid (100µL). Each sample was then vortexed for 1 minute, after which. a 2.5x volume of ice cold 100% ethanol was added (330µL) and the samples were incubated at -20ºC for 30 minutes. Samples were then centrifuged for 5 minutes at 13,000rpm and the supernatant discarded. A second volume of ice cold 100% ethanol (500µL) was added and the samples vortexed for 1 minute. This was followed by centrifugation for 10 minutes at 13,000rpm and the supernatant discarded. Samples were then dried for 30 minutes to evaporate any remaining ethanol. To resuspend the DNA and RNA,

100µL of TE^{-4} buffer was added to each sample and incubated for 15 minutes at 37ºC prior to downstream analysis.

Quantification of the extracted nucleic acids were determined using a Nanodrop 2000c spectrophotometer (Desjardins & Conklin, 2010). The optical surface was cleaned by pipetting 2µL of ddH_2O onto the lower optical surface and lowering the arm to ensure that the upper optical surface came into contact with the ddH_2O. A clean, lint free wipe was used to wipe both optical surfaces after cleaning and between each reading. The nucleic acid application was chosen in the nanodrop software and 2µL of TE^{-4} buffer read as the blank. The absorbance at 230nm (A230), 260nm (A260), and 280nm (A280) of both the DNA and RNA samples were read and the concentration calculated with the Nanodrop software, using the DNA-50 option to calculate the concentration of double stranded DNA (dsDNA) and RNA-40 option to calculate the concentration of RNA respectively. To determine the sample quality the ratio of A260/A280 was used with ~1.8 indicating pure DNA and ~2.0 indicating pure RNA. The overall spectral data was analyzed for additional absorbance between 220nm and 240nm to assess for phenolic contamination in the TRIzol® and acid-guanidinium extractions and residual guanidinium in the proteinase K and acid-guanidinium extractions (Desjardins & Conklin, 2010).

Prior to amplification all RNA samples were treated with 0.5µL of 1µg/µL DNase I and incubated at 37°C for 30 minutes to digest any remaining DNA. The samples were then incubated at 75°C for 10 minutes to deactivate the DNase (Huang, et. al., 1996).

2.2 Amplification and Sequencing

To assess the quality and quantity of DNA obtained, qPCR was run for 35 cycles using an ABI PRISM 7000 thermocycler and Qiagen QuantiNova SYBR Green PCR kit as per the manufacturer instructions using the high carboxy-X-rhodamine (ROX) concentration (1:10 dilution) as indicated for the ABI PRISM 7000 (Appendix C). Reverse transcriptase-quantitative PCR was used to further assess the quality and quantity of the RNA. To determine amplifiability, RT-qPCR was run for 35 cycles using an ABI PRISM 7000 thermocycler and Qiagen QuantiNova SYBR Green RT-PCR kit as per the manufacturer

instructions using the high ROX concentration (1:10 dilution) as indicated for the ABI PRISM 7000 (Appendix D). The combined annealing and extension time for both qPCR and RT-qPCR was adjusted from 10 seconds to 30 seconds per cycle due to the limitations of the ABI PRISM 7000 settings. For both qPCR and RT-qPCR, the previously authenticated β2M primers published by Harrington, et. al. (2007) were used in this research (Table 1). The GAPDH primers authenticated and published by Peuch et. al. (2015) were used to target the housekeeping gene (Table 1).

A subset of the amplified samples were sequenced to ensure the specificity of the primers and amplification. Primers, unincorporated nucleotides, enzymes, and salts were removed from the amplified samples using QIAquick PCR Clean Up kit, as per manufacturer instructions, to ensure sample purity. Sequencing was performed on an ABI 3130xl sequencer with 36cm capillary and performance optimized polymer (POP4) solid phase. A representative sample from each extraction type for each species was chosen based on the highest quantification and quality as determined by qPCR. For a total of 12 samples and 24 sequences, 12 forward and 12 reverse.

Table 1. Primer targets for qPCR amplification of cytokine and housekeeping genes for bovine, ovine, and odocoileus brain samples.

Target gene	Primer sequence (5' to 3')	Amplicon size	Conc (nM)
β2M	F- AGACACCCACCAGAAGATGG	98bp	700
	R- TCCCCATTCTTCAGCAAATC		700
GAPDH	F–ATCTCGCTCCTGGAAGATG	227bp	700
	R-TCGGAGTGAACGGATTCG		700

Note. The primers were designed for use with multiple species. The β2M primers were originally authenticated and published by Harrington et. al., (2007). The GAPDH primers were originally authenticaed and published by Puech et. al., (2015). Abbreviations. F: forward; R: reverse; bp: base pair; β2M: beta-2-microglobulin; GAPDH: Glyceraldehyde 3-phosphate dehydrogenase

2.3 Sample Quality Analysis

Efficiency and cycle threshold (Ct) values were determined using the common base method of analysis for paired samples (Ganger, et. al, 2017) as calculated by the ABI 7000 software. Using the Amplify 4 software, a PCR simulation was run for each set of primers, with the *Bos taurus* glyceraldehyde-3-phosphate dehydrogenase sequence ID: NM 001034034.2 from

the NCBI database, as the reference sample to generate an expected melting temperature for the GAPDH amplicon, 83°C. The *Bos taurus* beta-2-microglobulin sequence ID: XM_002691119.4 from the NCBI database, was used as the reference sample to generate the expected melting temperature for the β2M amplicon, 78°C. A melt curve was performed for each sample. This was compared to the expected melting temperature to determine the specificity of the reaction.

Secondary confirmation of specificity of the amplification was done by analysis of the sequencing data. Prior to analysis the electropherogram of each of the sequenced amplification products was visually verified for accuracy and data quality. SnapGene v5.2.4 was used to perform electropherogram editing, data clean up, and to align the edited sequences. Any ambiguous peak sequences were deleted from the ends, dye blobs and poorly resolved peaks accounted for, and determinations made on any internal ambiguous peaks to ensure the integrity of the data being analyzed. The edited sequences were then compared to the NCBI BLAST database to confirm amplification specificity. A query cover and percent identical score of greater than 95% were taken to be significant if accompanied by a low E score, indicating a low likelihood of another match occurring by chance within the database.

3.0 Results

3.1 Sample Preparation and Experimental Procedures

Spectrophotometric analysis showed a consistent A_{260}/A_{280} ratio for all DNA extracted with proteinase K from frozen samples and the positive control with the average ratio being 1.88 and ranging between 1.87 – 1.9 (Appendix E). These samples also showed effective extraction with an average concentration of 65ng/μL and a range of 18.3ng/μL – 94.5ng/μL. The average A_{260}/A_{280} for the FF and FFPE proteinase K extracted DNA samples was found to be 1.5 with a range of 1.13 – 1.85, and an average concentration of 3.94ng/μL, ranging from 3.0ng/μL – 6.7ng/μL. The sample labelled Cow FF 1 was not included in these calculations as the spectrophotometric data for this sample indicated no DNA present and an absorbance ratio of 0.55. This may indicate inhibition of the proteinase K enzyme during digestion or a very low yield which was lost during purification as some loss during this

process is common. The replicate Cow FF 2 yielded 3.5ng/μL and had an absorbance ratio of 1.85. The reagent negative showed a concentration of 73.7ng/μL with an A_{260}/A_{280} of 1.53. Among the animal cohorts the cow samples appeared to have the highest purity with an average A_{260}/A_{280} of 1.81 when averaged across all three preservation types.

The DNA extracted from frozen samples using TRIzol® had an average A_{260}/A_{280} absorbance ratio of 1.64, ranging between 1.55 – 1.76, and an average concentration of 128.7ng/μL, ranging from 84.5ng/μL – 207.1ng/μL. The average absorbance ratio of the FF and FFPE TRIzol® extracted DNA samples was 1.56, ranging between 1.55 – 1.58 with an average concentration of 98.14ng/μL, ranging from 77.1ng/μL – 118.1ng/μL. The reagent negative showed an absence of DNA with a concentration of -0.2ng/μL and an A_{260}/A_{280} of -0.05.

These data indicate that based on spectrophotometric analysis, both proteinase K and TRIzol® extraction methods were able to isolate DNA from all preservation types. The extracts from both methods had a sufficiently high indicator of purity and adequate yield DNA for qPCR analysis, with the exception of Cow FF1.

Spectrophotometric analysis of the acid-guanidinium phenol-chloroform extracted RNA from the frozen samples showed an average A_{260}/A_{280} ratio of 1.96, ranging between 1.84 – 2.05, and an average concentration of 64.95ng/μL, ranging between 25.7ng/μL – 146.1μL. The average absorbance ratio of the FF and FFPE acid-guanidinium phenol-chloroform extracted RNA was measured to be 1.67, ranging between 1.6 – 1.87, with an average concentration of 10.52ng/μL, ranging between 9.1ng/μL – 12.7ng/μL. The reagent negative showed an absence of RNA with a concentration of -1.8ng/μL and an A_{260}/A_{280} of 1.94.

The RNA extracted from frozen samples using TRIzol® had an average A_{260}/A_{280} of 1.92, with a range of 1.81 – 2.04, and an average concentration of 78.17ng/μL, ranging from 54.7ng/μL – 94.7ng/μL. The average absorbance ratio of the FF and FFPE TRIzol® extracted RNA samples was 1.81, with a range of 1.44 – 2.09, and an average concentration of 2.59, ranging from 2.0ng/μL – 3.4ng/μL.

These data indicate that based on spectrophotometric analysis, both acid-guanidinium thiocyanate phenol-chloroform and TRIzol® extraction methods were able to isolate RNA from all preservation types. The extracts from both methods had a sufficiently high indicator of purity and adequate yield RNA for RT-qPCR analysis,

3.2 Amplification and Sequencing

The DNA TRIzol® extraction had an overall failure rate of 16.67% with 6 out of 36 samples failing to show amplificaiton. This rate was not evenly distributed between the two amplicons. There was a single failure to amplify the β2M target and 5 failures to amplify the GAPDH target. The Sheep FFPE 1 sample was a common failure to both amplicons within the TRIzol® extracted samples, potentially indicating poor DNA preservation or ineffective nucleic acid isolation. The proteinase K extract had an overall failure rate of 50% with 18 out of 36 samples failing to show amplification. This rate was not evenly distributed between the 2 amplicons with the larger GAPDH amplicon failing to amplify in 77.78% of samples, 14 out of 18 samples, while the β2M amplicon had a 22.22% rate of failure, 4 out of 18 samples. Of the failed samples, 4 samples were common to both amplicons within the proteinase K extracted samples, possibly indicating poor DNA preservation or ineffective nucleic acid isolation. The TRIzol® extraction negative showed amplification in both the β2M target and the GAPDH target across 2 qPCR runs in 2 different plate locations, indicating possible cross contamination at the testing facility as the spectrophotometric data showed no nucleic acids present. No other DNA negatives or qPCR reagent negatives showed any detectable amplification.

The RNA TRIzol® extraction had an overall 27.78% failure rate. This rate was consistent between the β2M and GAPDH amplicons with 5 out of 18 samples in each set failing to show amplification, and 4 of the 5 failures in common between the two amplicons, indicating potential sample quality issues. The GuSCN RNA extraction had a 30.56% failure rate with 11 out of 36 samples failing to show detectable amplification. This rate was not consistent between the two amplicons with the smaller β2M amplicon having a 16.67% failure rate, 3 out of 18, and the larger GAPDH amplicon failing to amplify in 44.44% of the samples, 8 out of 18. Of the failed samples, 2 were common between the amplicons. No individual sample

failed across both extraction types and amplicons. The GuSCN extraction negative showed no amplification with the β2M primers, however this reagent negative showed amplification with the GAPDH primers across 3 RT-qPCR runs and 3 different locations within the plate, indicating possible contamination. No other RNA extraction negatives or PCR negatives showed amplification.

A representative subset, from both the DNA and RNA, was chosen from the amplified samples to be sequenced to verify primer specificitiy (Appendix H). Two samples from each species and preservation type were chosen, distributed evenly between the two target amplicons to ensure a representative sample. Where possible the sample with the lower Ct was used. Of the 24 sequences generated, 12 forward and 12 reverse, 5 RNA sequences and 3 DNA sequences were successful (Table 2). All succesful sequences were of the GAPDH amplicon and were predominantly TRIzol® extracted samples with 6 sequences from TRIzol® extraction and 2 from the GuSCN extraction. An additional GuSCN extraction was able to be read, however the sequence generated was too short to provide BLAST results and was thus discarded as unsuccessful.

3.3 Sample Quality Analysis

To assess the quality of each of the extracted samples, qPCR and RT-qPCR were used to amplify DNA and RNA respectively. A detectable Ct was taken to indicate a sample of amplifiable quality thereby indicating potential for use in further analysis. Duplicates from each of the extractions were amplified using 2 different sets of primers, 1 smaller and 1 larger, for a total of 24 samples, 12 per preservation method.

The frozen samples consistently showed good amplification with all but 2 frozen sample reactions amplifying successfully and all successful samples having a Ct of less than 31.67 (Appendix F). Of the 22 successfully amplified samples, 20 had a Ct lower than 26 cycles, and 11 of those had a Ct of less than 5 cycles. Both samples which failed to amplify were proteinase K extracted cow samples with the GAPDH amplicon target. The FF DNA samples showed a lower rate of success with 13 reactions amplifying successfully, of which 10 were TRIzol® extracted samples and 3 proteinase K extracted samples (Table 2). The average Ct,

for the FF samples, was 32.1 cycles with a range between 30.64 – 34.04 cycles. The FFPE samples had the same success rate as the FF samples, with 8 TRIzol® samples and 5 proteinase K samples successfully amplifying, however the difference in success rate between the groups could not be determined due to low sample number ($\chi^2 = 1.7529$, df = 2, p = 0.4163). The average Ct for the FFPE samples was 32.7 cycles, with a range between 30.91 – 34.13 cycles (Appendix F). The β2M amplicon showed a greater success rate with 30 out of 36 samples showing amplification, while the GAPDH amplicon was successfully amplified in 17 out of 36 reactions (Appendix F).

Table 2. qPCR amplification success by preservation method.

	Preservation		
Extraction	Frozen	Formalin Fixed	FFPE
TRIzol®	12	10	8
Proteinase K	10	3	5

For each preservation type, 12 samples were run with 2 replicates of each species. Successful amplification was determined based on detectable Ct, as calculated by ABI PRISM 7000 (Appendix F).

All of the frozen samples showed RNA amplification regardless of extraction method, while only half of the FF samples had a detectable Ct value. The FFPE samples appeared to show a higher success rate than the FF with 10 TRIzol® samples and 8 GuSCN samples showing amplification (Table 3). A Pearson's chi-squared test determined no significant difference between the 2 rates of success however due to low sample number this test my not be robust ($\chi^2 = 0.14378$, df = 2, p = 0.9306). There was comparable amplification between the two amplicons with 26 out of 36 samples showing amplification with the GAPDH target and 27 samples with the β2M target (Appendix G).

Table 3. RT-qPCR amplification success by preservation method.

	Preservation		
Extraction	Frozen	FF	FFPE
TRIzol®	12	6	10
GuSCN	12	5	8

For each preservation type, 12 samples were run with 2 replicates of each species. Successful amplification was determined based on detectable Ct, as calculated by ABI PRISM 7000 (Appendix G).

Frozen samples had consistently lower Ct values (Appendix G), indicating higher amounts of RNA, which is consistent with previous findings (Evers, et. al., 2011). A melt curve analysis was performed for all samples and compared to the expected melting temperature to determine the target specificity of amplification. For the β2M target, the proteinase K extracted DNA samples had an average melting temperature of 75.28°C, while the TRIzol® extracted DNA samples had an average melting temperature of 76.47°C (Table 4). For the GAPDH target, the proteinase K extracted DNA samples had an average melting temperature of 83.15°C, and the TRIzol® extracted DNA samples had an average melting temperature of 83.4°C (Table 4). The averages were calculated using only samples with a detectable Ct value (Appendix F).

Table 4. DNA qPCR Melt Curve by extraction method and target amplicon.

	TRIzol®		**Proteinase K**	
Expected melting temperature	Average melting temperature (°C)	Range	Average melting temperature (°C)	Range
β2M - 78°C	76.47	72 – 79.6	75.07	72.3 – 78.9
GAPDH - 83°C	83.4	82.8 – 83.8	83.15	82.5 – 83.8

Expected melting temperature was determined using *Bos taurus* GAPDH sequence ID: NM 001034034.2 and β2M sequence ID: XM_002691119.4 from the NCBI database with the Amplify4 software. Melt curve analysis was performed using ABI PRISM 7000 thermocycler. Range and averages were calculated using only samples with detectable Ct value (Appendix F).

For the β2M target, the TRIzol® extracted RNA samples had an average melting temperature of 78.23°C, while the GuSCN extracted RNA samples had an average melting temperature of 78.27°C (Table 5). For the GAPDH target, the TRIzol® extracted RNA samples had an average melting temperature of 83.35°C, and the GuSCN extracted RNA samples had an average melting temperature of 82.9°C (Table 5). The averages were calculated using only samples with a detectable Ct value (Appendix G).

Table 5. RNA RT-qPCR melt curve by extraction method and target amplicon.

	TRIzol®		GuSCN	
Expected melting temperature	Average melting temperature (°C)	Range	Average melting temperature (°C)	Range
β2M - 78°C	78.23	78 – 78.7	78.27	77.3 – 79.2
GAPDH - 83°C	83.35	82.7 – 83.9	82.9	82.5 – 83.4

Expected melting temperature was determined using *Bos taurus* GAPDH sequence ID: NM 001034034.2 and β2M sequence ID: XM_002691119.4 from the NCBI database with the Amplify4 software. Melt curve analysis was performed using ABI 7000 PRISM thermocycler. Range and averages were calculated using only samples with detectable Ct value (Appendix G).

A subset of 6 of each of the DNA and RNA amplified samples were sequenced to confirm the specificity of the target sequence. The subset was chosen with an even distribution of species, extraction method, and preservation type to ensure that it was representative of the overall sample set. A total of 24 sequences were generated, 12 forward and 12 reverse. Of the 12 DNA sequences generated 3 were successful. The TRIzol® extracted Deer F1 sample yielded both a successful forward and reverse sequence while the TRIzol® extracted Cow FFPE2 only yielded a successful forward sequence (Table 6). Of the 12 RNA sequences generated 5 were successful, with 3 being from TRIzol® extracted samples and 2 from GuSCN extracted samples. The TRIzol® extracted Deer FF2 sample yielded both a successful forward and reverse sequence, while the Cow FFPE1 only yielded a successful forward sequence. The GuSCN extracted Sheep F1 yielded both a successful forward and reverse sequence.

The successful sequences were searched on the NCBI database using the BLAST tool to identify the species of the target amplicon. The expected species appeared within the top results for all sequences with all sequences showing a greater than 97% identical sequence to the expected species (Table 6). In all instances where the percent identical was less than 100% the difference between the expected sequence and the amplified sequence was 1-2 base pairs (Appendix I).

Table 6. Sanger sequencing and NCBI BLAST match.

Sample ID	Direction	Extraction	NCBI BLAST ID	% Identical	E
Deer F 1	Forward	TRIzol® DNA	*Odocoileus virginianus texanus*	100	$2e^{-78}$
Deer F 2	Reverse	TRIzol® DNA	*Odocoileus virginianus texanus*	100	$4e^{-80}$
Cow FFPE 2	Forward	TRIzol® DNA	*Bos taurus*	100	$5e^{-58}$
Deer FF 2	Forward	TRIzol® RNA	*Odocoileus virginianus texanus*	100	$5e^{-79}$
Deer FF 2	Reverse	TRIzol® RNA	*Odocoileus virginianus texanus*	98.24	$3e^{-76}$
Cow FFPE 1	Forward	TRIzol® RNA	*Bos taurus*	98.74	$2e^{-72}$
			**Odocoileus virginianus texanus*	99.37	$5e^{-74}$
Sheep F 1	Forward	GuSCN RNA	*Ovis aries*	97.13	$1e^{-75}$
			**Bos taurus*	98.85	$1e^{-80}$
Sheep F 1	Reverse	GuSCN RNA	*Ovis aries*	97.14	$1e^{-58}$
			***Syncerus caffer*	97.88	$3e^{-60}$

All successful sequences were of the GAPDH amplicon (227bp). See Appendix I for full sequences and complete list of NCBI BLAST matches.
*Where samples had a different match than the expected species, the expected species is listed first, with the top match listed second. In all cases the discrepancy is 1-2 base pair difference between the top match and the expected species.
**The lab in which samples were processed has never processed any samples of *Syncerus caffer*.

4.0 Discussion

The aim of this study was to assess the efficacy of the TRIzol® reagent for the simultaneous extraction of RNA and DNA from archived biomedical brain samples. To perform this assessment, three animal brain samples were acquired, through donation, for this research. While the most reliable archived biomedical samples are obtained antemortem, such as during surgery, this is frequently not possible with tissue such as brains or non-biopsy samples. These samples are often taken during autopsy which can occur anywhere between 6 hours and several days after death. To reduce post-mortem degradation, the criteria for selection of brain samples for this research was met if the interval between death and sample

acquisition was less than 72 hours. A tissue fixation was performed using a buffered 10% formalin solution. Although fixation solution concentrations are not standardized and can vary widely, a 10% solution was chosen as this is the most commonly used concentration for tissue fixation (Wang et. al., 2013). Samples were fixed for 48 hours as the standard recommendation is 1 hour per millimetre of sample thickness, however fixation times can vary from 2 to several days (Spencer, et. al., 2013; Evers, et. al., 2011). Similarly, there is little consensus within the literature as to which deparaffinization method is best or if deparaffinization is required. Xylene and heating are the two most employed methods to removing paraffin (Coombs, et. al, 1999; Wang, et. al, 2013). For this study a xylene deparaffinization was used with a heating step at the end. The heat step was perfromed at a reduced temperature to minimize hydrolytic damage while still reversing crosslinks and melting residual paraffin.

Two reference genes, GAPDH and β2M were chosen as qPCR amplification targets for all three species. These two sets of primers used have been previously verified, by Harrington et. al. (2007) and Puech et. al. (2015) respectively, and shown to be effective across multiple species including the species used in this study. Additionally, these primers were chosen as they provide both a short and moderate amplicon size to determine nucleic acid quality and assess potential damage. Prior to qPCR quality analysis, spectrophotometric analysis indicated that the proteinase K extracted DNA had a high purity, A_{260}/A_{280} ratio 1.87 – 1.9, and all samples, with the exception of Cow FF 1, were measured to have DNA quantities within the expected range. Despite the high purity and high DNA yield detected by the Nanodrop spectrophotometer, the proteinase K samples showed the highest rate of failure during qPCR with 77.78% of the GAPDH amplicon failing to show amplification and the β2M target failing to amplify in 22.2% of samples. The TRIzol® extracted DNA, which was measured to have an average A_{260}/A_{280} ratio of 1.64, showed a higher rate of amplification with only 16.67% of the samples failing. The higher rate of failure of the GAPDH amplicon was expected as a larger amplicon is more likely to experience crosslinking, base modifications, and strand breaks (Do & Dobrovic, 2015). Given the relatively high rate of success, the lower A_{260}/A_{280} ratio found in the TRIzol® samples may be attributable to

residual phenol which absorbs at 270nm as noted in previous studies (Doshii, et. al., 2009) (Hummon, et. al., 2007).

The higher failure rate observed in the proteinase K digests, compared to the TRIzol® extraction, may be due to secondary damage to the DNA during peptide bond hydrolysis. If proteinase K hydrolyzes a peptide bond in a location where DNA/protein crosslinking has occurred it may cause damage to the DNA resulting in a strandbreak. It is also possible that the TRIzol® was more efficient at formalin removal resulting in less inhibition during qPCR. Because spectrophotometry cannot distinguish between small fragments of DNA and long strands the purity and quantity readings from this analysis are used only as a screening tool, and not as a point of comparison.

Spectrophotometric analysis of the proteinase K negative indicated the presence of a DNA with a concentration of 73.7ng/μL. The low A_{260}/A_{280} ratio indicates that this is likely due to residual reagents or because absorbance is measured on a curve, overlap from protein absorbance in the 280nm wavelength. This sample also showed no amplification in downstream quality control analysis, such as qPCR, indicating that this reading is likely not due to the presence of DNA. This also highlights why spectrophotometry is used only as an initial screening tool for the more accurate downstream analyses such as qPCR.

Spectrophotometric analysis of the RNA extracts indicated a high purity, with an average A_{260}/A_{280} ratio of 1.96 and 1.92 for the GuSCN and TRIzol® extractions respectively. Both extraction methods had similar rates of RT-qPCR failure at 30.56% and 27.78% respectively. While the expected higher rate of GAPDH target failure was seen in the GuSCN extracted samples the TRIzol® samples had the same rate of success regardless of the amplicon size.

The mode of preservation used must also be considered when determining the rate of success. Frozen samples are considered the preferred method of storage for nucleic acid research. This is consistent with our findings, where all the frozen samples for both the DNA and RNA extractions showed good amplification, with the exception of the two proteinase K extracted cow samples, (Table 2 and Table 3). The spectrophotometric analysis of these two samples indicated a high purity as well as sufficient DNA (Appendix E), indicating that the

DNA may have undergone degradation due to the archival storage period as samples were stored at -20°C prior to extraction as opposed to the optimal -80°C. The FF and the FFPE samples extracted by TRIzol® showed a high rate of success with 10 of 12 FF and 8 of 12 FFPE showing amplification as compared to the 3 of 12 FF and 5 of 12 FFPE extracted by the proteinase K method. Unfortunately, this study was not robust enough to determine if this was a significant difference due to the small sample size. However, this trend may prove to be significant in a larger study. Our results for the FFPE samples are consistent with a study by Funabashi, et. al., (2012) that looked at FFPE samples that had been stored for 3-12 years and found a higher rate of success using a similar organic solvent extraction method, phenol-chloroform separation, to isolate DNA, as compared to a salting out method.

When examining the two RNA extraction methods in combination with preservation media both the TRIzol® and GuSCN extracted FF and FFPE samples showed a similar success rate as observed in previous studies. A Pearson's correlation of the two methods of extraction, controlling for preservation type, showed that there was no significant difference in the rate of success observed between the two methods, with the caveat that due to small sample sizes this finding may not carry forward to larger studies..

To determine the specificity of the amplification, a melt curve was performed, with the reference temperature determined using *Bos taurus* sequence IDs: NM 001034034.2 and XM_002691119.4. All successfully amplified DNA samples showed a melt curve within the expected range for the target amplicon (Table 4 and Table 5). The RNA samples showed a tighter amplification curve with a narrower range than the DNA results. However, the larger variation in the DNA melt curves may be due to a lowered specificity as the amplicons chosen were originally optimized for RNA (Harrington, et. al., 2007; Puech, et. al., 2015). It may also indicate the variation and differences in preservation.

The specificity of the amplification products was confirmed by Sanger sequencing with only the GAPDH targets sequencing with accuracy. Of the successful sequences, the RNA samples yielded nearly double the number of sequences (Table 6). The NCBI BLAST results of the DNA sequences showed 100% identical match with very low E score indicating that the match was extremely unlikely to be due to chance. The RNA sequences showed some

variation in the BLAST matches with 3 of the 5 sequences having a closer match with a species other than the expected. Of the potentially confounding matches, 2 were for species also included in this study. The Sheep F1 reverse sequence matched with a species which has not been processed in either the extraction lab or the testing lab which performed the RT-qPCR and sequencing. The GAPDH protein is highly conserved across species, however it is well documented that formalin fixation can induce deamination resulting in C:T base shifts, G:A base shifts, and abasic sites into which adenine will preferrentially be incorporated (Robbe, et. al., 2018; Srinivasan, et. al., 2002). These considerations may help to explain the variation observed in the Cow FFPE 1 sample, but they can not be applied to the Sheep F1 samples as this sample did not undergo formalin fixation. Hydrolytic damage, however, can also cause deamination which may account for a large portion of the variation observed in the Sheep F1 sequences as the rate of G:A shift and C:T shift is high (Appendix I). This is particularly true with multiple freeze thaw cycles (Wang, et. al., 2015). Given that all samples underwent at least 2-3 freeze thaw cycles, it is likely that the sequence variation observed can be at least partially accounted for as RNA damage and not mutations.

Despite the difficulties involved with using FF and FFPE tissues, these results show that the potential for research on these samples is high, and indicates that optimization of a multiomic extraction method makes further research into this possiblity worthwhile. This study found no significant difference in the number of successful samples between a traditional extraction method and the TRIzol® triple extraction. With the caveat that sample sizes were low, it appears that overall TRIzol® performed as well as, if not better than, the traditional methods. The results of this study suggest that TRIzol® may provide a reliable, quick, and simplistic method of obtaining high quality RNA and DNA data from a single FFPE or FF sample. This method is also more cost effective as there is reduced need for chemical inventory. It also requires less handling of hazardous chemicals during reagent preparation, increasing technician safety. Additionally, there is the potential to obtain proteomic information from the same set of samples, however investigation of the viability for this was beyond the scope of this study.

While not a focus of this study, it was observed that there may be evidence for a higher rate of RNA preservation in FFPE samples compared to that of DNA. This may be due to the

differences in DNA and RNA structure. Formalin is known to induce methylene bridges by way of electrophilic attack on amine bases (Srinivasan, et. al., 2002). Formalin will also rapidly oxidize, producing an acidic environment. While DNA is generally more stable than RNA within the body's more basic environment, RNA has been shown to be more stable within an acidic environment. This difference in hydrophilicity is the property which both the GuSCN and TRIzol® reactions take advantage in order to separate DNA from RNA and may provide the chemical basis for the higher rate of successful amplifcation observed in the RNA extractions (Chomczynski & Sacchi, 1987). More research to verify this is needed before any conclusions can be drawn as the increase observed was small and the sample size is not large enough to measure significance.

5.0 Conclusion

The research potential for using FFPE tissue to study rare and difficult to obtain samples is immense. There have been a number of studies to determine the best method of accessing the DNA and RNA data held within these types of archived samples. However, there is little consensus as to which method is more effective, and comparatively little research has been done to obtain both sets of data from the same sample. As multiomic approaches to disease become more commonplace the ability to obtain both sets of data from a single source becomes more urgent. This study demonstrates that there is no significant difference between the efficacy of the current traditional methods being used and a TRIzol® triple extraction to obtain high quality DNA and RNA from frozen, formalin fixed, or formalin-fixed paraffin-embedded brain samples which have been stored for three years.

7.0 References

Altschul, S., Gish, W., Miller, W., Myers, E., & Lipman, D. (1990). Basic local alignment search tool. *Journal of Molecular Biology, 215*, 403-410.

Baltimore, D., Huang, A., & Stampfer, M. (1970). Ribonucleic acid synthesis of vesicular stomatitis virus, II. An RNA polymerase in the virion. *Proceedings of the National Academy of Sciences, 66*(2), 572-576.

Boom, R., Sol, C., Salimans, M., Jansen, C., Dillen, P. W.-v., & Noordaa, J. v. (1990). Rapid and simple method for purification of nucleic acids. *Journal of Clinical Microbiology, 28*, 495-503.

Castelhano, M., Acland, G., Ciccone, P., Corey, E., Mezey, J., Schimenti, J., & Todhunter, R. (2009). Development and use of DNA archives at veterinary teaching hospitals to investigate the genetic basis of disease in dogs. *Journal of American Veterinary Medical Association, 234*(1), 75-80.

Chen, B., Costantino, H., Liu, J., Hsu, C., & Shire, S. (1999). Influence of calcium ions on the structure and stability of recombinant human deoxyribonuclease I in the aqueous and lyophilized states. *Journal of Pharmaceutical Sciences, 88*(4), 477-482.

Chomcyzynski, P., & Sacchi, N. (2006). The single-step method of RNA isolation by acid guanidinium thiocyanate-phenol-chloroform extraction: twenty-something years on. *Nature Protocols, 1*, 581-585.

Chomczynski, P. (1993). A reagent for the single-step simultaneous isolation of RNA, DNA, and proteins from cell and tissue samples. *BioTechniques, 15*, 532-535.

Chomczynski, P., & Sacchi, N. (1987). Single-step method of RNA isolation by acid guanidinium thiocyanate-phenol-chloroform extraction. *Analytical Biochemistry, 162*, 156-159.

Churko, J., Mantalas, G., Snyder, M., & Wu, J. (2013). Overview of High Throughput Sequencing Technologies to Elucidate Molecular Pathways in Cardiovascular Diseases. *Circulation Research, 112*, 1613-1623.

Claussnitzer, M., Cho, J., Collins, R., Cox, N., Dermitzakis, E., Hurles, M., . . . McCarthy, M. (2020). A brief history of human disease genetics. *Nature, 577*(7789), 179-189.

Coombs, N., Gough, A., & Primrose, J. (1999). The Effect of Formaldehyde Fixation on RNA Optimization of Formaldehyde Adduct Removal. *Nucleic Acids Research, 27*(16), e12.

Cummings, T., Strum, J., Yoon, L., Szymanski, M., & Hulette, C. (2001). Recovery and Expression of Messenger RNA from Postmortem Human Brain Tissue. *Modern Pathology, 14*, 1157–1161.

Desjardins, P., & Conklin, D. (2010). NanoDrop Microvolume Quantitation of Nucleic Acids. *Journal of Visual Experiments*(45), e2565.

Do, H., & Dobrovic, A. (2015). Sequence Artifacts in DNA from Formalin-Fixed Tissues: Causes and Strategies for Minimization. *Clinical Chemistry, 61*(1), 64-71.

Doshii, R., Day, P., & Tirelli, N. (2009). Dissolved oxygen alteration of the spectrophotometric analysis and quantification of nucleic acid solutions. *Biochemical Society Transactions, 37*, 466-470.

Ebeling, W., Hennrich, N., Klockow, M., Metz, H., Orth, H., & Lang, H. (1974). Proteinase K from Tritirachium album Limber. *European Journal of Biochemistry, 47*(1), 91-97.

Esteve-Codina, A., Arpi, O., Martinez-García, M., Pinda, E., Mallo, M., Gut, M., & Balaña, .. C. (2017). A Comparison of RNA-Seq Results from Paired Formalin-Fixed Paraffin-Embedded and Fresh- Frozen Glioblastoma Tissue Samples. *PLoS One, 12*(1), e0170632.

Evers, D., Fowler, C., Cunningham, B., Mason, J., & O'Leary, T. (2011). The Effect of Formaldehyde Fixation on RNA: Optimization of Formaldehyde Adduct Removal. *The Journal of Molecular Diagnostics, 13*(3), 282-288.

Fabre, A., Colotte, M., Luis, A., Tuffet, S., & Bonnet, J. (2014). An efficient method for long-term room temperature storage of RNA. *European Journa of Human Genetics, 22*, 379-385.

Fox, C., Johnson, F., J, W., & Roller, P. (1985). Formaldehyde Fixation. *J Histochem Cytochem, 33*(8), 845-853.

Fraser, Z., Yoo, C., Sroya, M., Bellora, C., DeWitt, B., Sanchez, I., . . . Matheison, W. (2020). Effect of Different Proteinase K Digest Protocols and Deparaffinization Methods on Yield and Integrity of DNA Extracted From Formalin-fixed, Paraffin-embedded Tissue. *Journal of Histochemistry and Cytochemistry, 68*(3), 171-184.

Funabashi, K., Barcelos, D., Visoná, I., Sousa-e-Silva, M., Oliviera-e-Sousa, M., de-Franco, M., & Iwamura, E. (2012). DNA extraction and molecular analysis of non-tumoral liver, spleen, and brain from autopsy samples: The effect of formalin fixation and paraffin embedding. *Pathology - Research and Practice, 208*, 584-591.

Ganger, M., Dietz, G., & Ewing, S. (2017). A common base method for analysis of qPCR data and th applicaiton of simple blocking in qPCR experiments. *BMC Bioinformatics, 18*(534).

Gebert, L., & MacRae, I. (2019). Regulation of microRNA function in animals. *Nature Reviews Molecular Cell Biology, 20*, 21-37.

Gusella, J., Conneally, N., Naylor, P., Anderson, S., Tanzi, M., Watkins, R., . . . Martin, J. (1983). A polymorphic DNA marker genetically linked to Huntington's disease. *Nature, 306*, 234-238.

Harrington, N., Surujballi, O., Waters, W., & Prescott, J. (2007). Development and Evaluation of a Real-Time Reverse Transcription-PCR Assay for Quantification of Gamma Interferon mRNA To Diagnose Tuberculosis in Multiple Animal Species. *Clinical and Vaccine Immunology, 14*(12), 1563–1571.

Higuchi, R., Dollinger, G., Walsh, P., & Griffith, R. (1992). Simultaneous Amplification and Detection of Specific DNA Sequences. *Nature Biotechnology, 10*, 413-417.

Hilz, H., Wiegers, U., & Adamietz, P. (1975). Stimulation of proteinase K action by denaturing agents: application to the isolation of nucleic acids and the degradation of 'masked' proteins. *European Journal of Biochemistry, 56*(1), 103-108.

Huang, Z., Fasco, M., & Kaminsky, L. (1996). Optimization of Dnase I removal of contaminating DNA from RNA for use in quantitative RNA-PCR. *Biotechniques, 20*(6), 1012-1014.

Hummon, A., Lim, A., & Difilippantonio, M. (2007). Isolation and solubilization of proteins after TRIzol extraction of RNA and DNA from patient material follow a prolonged storage. *BioTechniques, 42*, 467-472.

IHC World. (n.d.). *Standard Protocol for Formalin-Fixed Paraffin Embeded Tissue.* Retrieved from stmichaelshosptial.com: http://www.stmichaelshospital.com/research/facilities/images/histology-methods-formalin-fixed-paraffin-embedded-tissue.pdf

Invitrogen. (2016). *ThermoFisher Scientific TRIzol Reagent User Guide.* Retrieved from ThermoFisher Scientific: https://www.thermofisher.com/document-connect/document-connect.html?url=https%3A%2F%2Fassets.thermofisher.com%2FTFS-Assets%2FLSG%2Fmanuals%2FMAN0016385_TRIzol_Reagent_DNA_Isol_UG.pdf&title=VXNlciBHdWlkZSAtIFRSSXpvbCBSZWFnZW50IC0gRXhwZXJpbWVudGFsIHByb3RvY2

Khan, M., Wu, J., Liu, B., Cheng, C., Akbar, M., Chai, Y., & Memon, A. (2018). Fluorescence and photophysical properties of xylene isomers in water: with experimental and theoretical approaches. *Royal Society Open Science, 5*, 171719.

Kim, S., Park, C., Ji, Y., Kim, D., Bae, H., Vrancken, M. v., . . . Kim, K.-M. (2017). Deamination Effects in Formalin-Fixed, Paraffin-Embedded Tissue Samples in the Era of Precision Medicine. *The Journal of Molecular Diagnostics, 19*(1), 137-146.

Kim, Y., Choi, E., Son, B., Seo, E., Lee, E., Ryu, J., & Lee, .. K. (2011). Effects of Storage Buffer and Temperature on the Integrity of Human DNA. *Korean Journal of Clinical Laboratory Sciences, 44*(1), 24-30.

Morris, K. (2011). The emerging role of RNA in the regulation of gene transcription in human cells. *Seminars in Cell and Developmental Biology, 22*(4), 351-359.

O'Brien, J., & Sampson, E. (1965). Lipid composition of the normal human brain: gray matter, white matter, and myelin*. *Journal of Lipid Research, 6*(4), 537-544.

Puech, C., Dedieu, L., Chantal, I., & Rodrigues, V. (2015). Design and evaluation of a unique SYBR Green real-time RT-PCR assay for quantification of five major cytokines in cattle, sheep and goats. *BMC Veterinary Research, 11*, 65.

Rio, D., Ares, M., Hanoon, G., & Nilsen, T. (2010). Ethanol Precipitation of RNA and the Use of Carriers. *Cold Spring Harbor Protocols, 6*.

Robbe, P., Popitsch, N., Knight, S., Antoniou, P., Becq, J., He, M., & Schuh, .. A. (2018). Clinical whole-genome sequencing from routine formalin-fixed, paraffin-embedded specimens: pilot study for the 100,000 Genomes Project. *Genetics in Medicine, 20*(10), 1196-1205.

Rychlik, W., Spencer, W., & Rhoads, R. (1990). Optimization of the annealing temperature for DNA amplification in vitro. *Nucleic Acids Research, 18*(21), 6409-6412.

Sölen, G., Edgren, M., Scott, O., & Révész, L. (1990). Radiosensitization by oxygen and radioprotection by thiols: analysis of the combined action according to a modified competition model. *International Journal of Radiation Biology, 57*(5), 959-969.

Saiki, R., Gelfand, D., Stoffl, S., Scharf, S., Higuchi, R., Horn, G., . . . Erlich, H. (1988). Primer-directed enzymativ amplificaiton of DNA with a thermostable DNA polymerase. *Science, 239*(4839), 487-491.

Saiki, R., Scharf, S., Faloona, F., Mullis, K., Horn, G., Erlich, H., & Arnheim, N. (1985). Enzymatic amplification of beta-globin genomic sequences and restriction site analysis for diagnosis of sickle cell anemia. *Science, 230*(4732), 1350-1354.

Sandberg, R., Yasuda, R., Pankratz, D., Carter, T., DelRio, J., Wodicka, L., . . . Barlow, C. (2000). Regional and strain-specific gene expression mapping in the adult mouse brain. *PNAS, 97*(20), 11038-11043.

Sanger, F., Nicklen, S., & Coulson, A. (1977). DNA sequencing with chain-terminating inhibitors. *Proceedings of the National Academy of Science USA, 74*(12), 5463-5467.

Shi, S., Datar, R., Liu, C., Wu, L., Zhang, Z., Cote, R., & Taylor, C. (2004). DNA extraction from archival formalin-fixed, paraffin-embedded tissues: heat-induced retrieval in alkaline solution. *Histochemistry and Cell Biology, 122*(3), 211-218.

Soverchia, L., Ubaldi, M., Leonardi-Essmann, F., Ciccocioppo, R., & Hardiman, G. (2005). Microarrays – The Challenge of Preparing Brain Tissue Samples. *Addiciton Biology, 10*(1), 5-13.

Spencer, D., Sehn, J., Abel, H., Watson, M., Pfeifer, J., & Duncavage, E. (2013). Comparison of Clinical Targeted Next-Generation Sequence Data from Formalin-Fixed and Fresh-Frozen Tissue Specimens. *The Journal of Molecular Diagnostics, 15*(5), 623-633.

Srinivasan, M., Sedmak, D., & Jewell, S. (2002). Effect of fixatives and tissue processing on the content and integrity of nucleic acids. *The American Journal of Pathology, 161*(6), 1961-1971.

Titford, M. (2006). A Short History of Histopathology Technique. *J Histotechnol, 29*(2), 99-110.

Tsanev, R., & Markov, G. (1960). Substances interfering with spectrophotometric estimation of nucleic acids and their elimination by the two-wavelength method. *Biochimica et Biophysica Acta, 42*, 442-452.

Wang, J., Gouda-Vossos, A., Dzamko, N., Halliday, G., & Huang, Y. (2013). DNA extraction from fresh-frozen and formalin-fixed, paraffinembedded human brain tissue. *Neuroscience Bulletin, 29*(5), 649-654.

Wang, Y., Zheng, H., Chen, J., Zhong, X., Wang, Y., Wang, Z., & Wang, Y. (2015). The Impact of Different Preservation Conditions and Freezing-Thawing Cycles on Quality of RNA, DNA, and Proteins in Cancer Tissue. *Biopreservation and Biobanking, 13*(5), 335-347.

Appendix A

Modified Formalin Fixation and Paraffin embedding protocol (IHC World)

1. In a 50mL Fix 2cm x 3cm block of tissue in 20mL volume of 10% buffered formalin for 24 hours at room temperature
2. Decant formalin and repeat step 1 with fresh formalin
3. To dehydrate and paraffin embed tissue process as follows:
    a. 70% ethanol, two changes, 1 hour each
    b. 80% ethanol, one change, 1 hour
    c. 95% ethanol, one change, 1 hour
    d. 100% ethanol, three changes, 1.5 hours each
    e. Xylene, three changes, 1.5 hours each
    f. Paraffin wax (58-60°C), two changes, 2 hours each
4. Decant paraffin, cap 50mL conical tube, and store at room temperature.

To Deparaffinize and rehydrate

1. Using a disposable scalpel and sterile tweezers remove a 1mm x 1mm section of FFPE tissue
2. Transfer to a sterile 2mL microcentrifuge tube
3. Deparaffinize and rehydrate as follows:
    a. Xylene, three changes, 10 minutes each
    b. 100% ethanol, two changes, 3 minutes each
    c. 95% ethanol, one change, 2 minutes
    d. 80% ethanol, one change, 2 minutes
    e. 75% ethanol, one change, 1 minute
    f. 50% ethanol, one change, 1 minute
    g. 1mL distilled water, incubate at 70°C for 10 minutes
    h. Incubate at -20 for 10 minutes
    i. Remove any remaining paraffin from top of water
    j. Decant water and transfer tissue to new sterile 2mL microcentrifuge tube.

Appendix B

TRIzol® Protocol (Invitrogen, 2016)

General guidelines

- Perform all steps at room temperature (20-25°C) unless otherwise noted.
- Use DEPC treated water to make reagents
- Ensure all non-disposable items are decontaminated with RnaseZap™, including centrifuges, pipettes, and work surfaces.
- Use Rnase and Dnase free barrier pipette tips
- UV sterilize hood, pipettes, pipette tip boxes, and sterilized tools, such as tweezers; pestles; and dental picks, for 20 minutes prior to beginning extraction
    - Keep tools in sterilization pouches and flip pouch halfway through Uving

Lyse sample

1. With sample in a sterile 2mL microcentrifuge tube, add 500µL of TRIzol® and homogenize with a disposable pestle
2. Add an additional 500µL of TRIzol® and homogenize
3. Centrifuge lysate for 5 minutes at 12,000 x g at 10°C and transfer clear supernatant to sterile 2mL microcentrifuge tube
4. Incubate for 5 minutes
5. Add 0.2mL chloroform and close tube
6. Incubate for 3 minutes
7. Centrifuge for 15 minutes at 12,000 x g at 4°C
    a. Phases should appear as a lower red phenol/chloroform phase with a clear colourless upper aqueous phase. If phases order is reversed, gently invert tube twice and allow to sit at room temperature for 5 minutes. This should cause phase order to correct.
8. Transfer the upper aqueous phase containing the RNA to a new sterile 2mL microcentrifuge tube.
    a. Avoid touching or transferring interphase or organic phase

Aqueous upper phase moves to RNA isolation

Organic phase moves to DNA isolation

RNA Isolation

1. Add 0.5mL isopropanol to the aqueous phase
2. Incubate for 10 minutes
3. Centrifuge for 10 minutes at 12,000 x g at 4°C
4. Discard supernatant with a micropipette being careful not to disturb pellet
5. Resuspend pellet in 1mL of 75% ethanol
6. Vortex sample for 15 seconds to ensure resuspension
7. Centrifuge for 5 minutes in microcentrifuge
8. Discard supernatant with a micropipette being careful not to disturb pellet
9. Air dry RNA pellet for 10 minutes or until no visible ethanol remains in tube
10. Resuspend RNA in 100µL TE^{-4} buffer, pH 8.0, by pipetting up and down
11. Incubate at 56°C for 15 minutes
12. Quantify using Nanodrop 2000c
13. Use Ethanol precipitation for addition purification.

DNA Isolation

1. Remove any aqueous phase remaining
2. Add 0.3mL of 100% ethanol
3. Cap tube and invert several times
4. Incubate 3 minutes
5. Centrifuge for 5 minutes at 2,000 x g at 4°C to pellet DNA
6. Transfer phenol-ethanol supernatant to new tube for protein isolation
7. Resuspend the DNA pellet in 1mL of 0.1M sodium citrate in 10% ethanol, pH 8.5
8. Incubate for 30 minutes gently inverting occasionally
9. Centrifuge for 5 minutes at 2,000 x g at 4°C
10. Discard supernatant with micropipette being careful not to disturb pellet
11. Repeat steps 7-10 once
12. Resuspend the pellet in 1.5mL of 75% ethanol

13. Incubate for 20 minutes gently inverting occasionally
14. Centrifuge for 5 minutes at 2,000 x g at 4°C
15. Discard supernatant with micropipette being careful not to disturb pellet
16. Air dry the DNA pellet for 10 minutes
17. Resuspend in 100µL TE^{-4}, pH 8.0 by pipetting up and down
18. Quantify using Nanodrop 2000c
19. Use ethanol precipitation for additional purification

Appendix C

QuantiNova SYBR Green PCR kit

Uses high ROX concentration as per QuantiNova manufacturer instructions for use with ABI 7000

Appendix Table 1. qPCR Master Mix set up parameters.

Reagent	β2M	GAPDH
2x QuantiNova SYBR Green Master Mix	10µL	10µL
ROX reference dye	2.0µL	2.0µL
Forward Primer (0.1mM)	0.1µL Final con'c (700nM)	0.1µL Final con'c (700nm)
Reverse Primer (0.1mM)	0.1µL Final con'c (700nM)	0.1µL Final con'c (700nm)
RNAse Free Water	2.8µL	2.8µL
Template DNA	5.0µL	5.0µL
Total Volume	20µL	20µL

Appendix Table 2. qPCR running parameters.

Step	Time	Temperature	Ramp Rate
PCR initial Activation Set up	2 min	95°C	Maximal/Fast Mode
2-Step Cycling			
Denaturation	5s	95°C	Maximal/Fast Mode
Combined Annealing/Extension	30s*	60°C	Maximal/Fast Mode
Number of Cycles	35		
Melt Curve Analysis	As per User Manual		

*Altered from QuantiNova manufacturer instructions (10s) to accommodate ABI 7000 minimum time requirement.

Appendix D

QuantiNova SYBR Green RT-PCR kit

For primers make a 10x total concentration master mix for each. A 10x primer mix consists of final concentration of 5 μM forward primer and 5 μM reverse primer.
Reverse primer

Primers for use in RT-qPCR
GAPDH
β2M

Uses high ROX concentration as per QuantiNova manufacturer instructions for use with ABI 7000

Appendix Table 3. RT-qPCR Master mix set up parameters.

	Volumes
2x QuantiNova SYBR Green Master Mix	10μL
ROX reference dye	1.0μL
QN SYBR Green RT Mix	0.2μL
10x Primer Mix	2.0μL
RNAse Free Water	1.8μL
Template DNA	5.0μL
Total Volume	**20μL**

Appendix Table 4. RT-qPCR running parameters.

Step	**Time**	**Temperature**	**Ramp Rate**
Reverse Transcription	10 min	50°C	Maximal/Fast Mode
PCR initial Activation Set up	2 min	95°C	Maximal/Fast Mode
2-Step Cycling			
Denaturation	5s	95°C	Maximal/Fast Mode
Combined Annealing/Extension	30s*	60°C	Maximal/Fast Mode
Number of Cycles	35		
Melt Curve Analysis	As per User Manual		

*Altered from QuantiNova manufacturer instructions (10s) to accommodate ABI 7000 minimum time requirement.

Appendix E

	DNA Proteinase K		DNA TRIzol®		RNA GuSCN		RNA TRIzol®	
	ng/μL	A260/A280	ng/μL	A260/A280	ng/μL	A260/A280	ng/μL	A260/A280
SheepFFPE1	3.4	1.61	86.1	1.56	9.9	1.66	2.7	2.04
SheepFFPE2	3.5	1.59	87.3	1.56	10.4	1.64	2.4	1.83
SheepFF1	3	1.39	77.1	1.55	8.8	1.65	2.7	1.44
SheepFF2	3.3	1.41	83.8	1.55	12.7	1.73	2.5	1.61
SheepF1	94.5	1.89	108.1	1.61	59.8	2.05	92.8	1.81
SheepF2	90.5	1.88	88.8	1.58	146.1	2.02	73.8	1.81
DeerFFPE1	3.4	1.39	107.2	1.58	9.5	1.62	3.4	1.82
DeerFFPE2	3.7	1.47	95.7	1.56	9.1	1.73	2.8	1.91
DeerFF1	6.7	1.13	95.6	1.55	10.8	1.66	2.6	1.86
DeerFF2	5	1.31	102.9	1.56	8.8	1.61	2.3	1.71
DeerF1	86.1	1.9	84.5	1.55	25.7	1.84	90.3	1.91
DeerF2	88.9	1.9	168	1.76	36	1.92	58.7	1.94
CowFFPE1	4.3	1.71	109.7	1.56	11.2	1.72	2.2	1.67
CowFFPE2	3.6	1.69	106.2	1.55	10.4	1.6	2	2.09
CowFF1	-1.3	0.55	118.1	1.56	12.6	1.62	2.6	1.87
CowFF2	3.5	1.85	108	1.57	12	1.87	2.9	1.94
CowF1	18.3	1.89	116.1	1.58	71.8	1.97	98.7	2.02
CowF2	29.4	1.87	207.1	1.75	50.3	1.94	54.7	2.04
positive control	47.3	1.88						
negative	73.7	1.53	-0.2	1.03	-1.8	1.94	-	-
	Average ng/μL	**Average A_{260}/A_{280}**	**Average ng/μL**	**Average A_{260}/A_{280}**	**Average ng/μL**	**Average A_{260}/A_{280}**	**Average ng/μL**	**Average A_{260}/A_{280}**
F Cow	23.85	1.88	161.6	1.665	61.05	1.955	76.7	2.03
F Deer	87.5	1.9	126.25	1.665	30.85	1.88	74.5	1.925
F Sheep	92.5	1.885	98.45	1.595	102.95	2.035	83.3	1.81
FF Cow	3.5	1.85	113.05	1.565	12.3	1.745	2.75	1.905
FF Deer	5.85	1.22	99.25	1.555	9.8	1.635	2.45	1.785
FF Sheep	3.15	1.4	80.45	1.55	10.75	1.69	2.6	1.525
FFPE Cow	3.95	1.7	107.95	1.555	10.8	1.66	2.1	1.88
FFPE Deer	3.55	1.43	101.45	1.57	9.3	1.675	3.1	1.865
FFPE Sheep	3.45	1.6	86.7	1.56	10.15	1.65	2.55	1.935
Frozen	65	1.887	128.76	1.638	64.95	1.956	78.16	1.92
Fixed	3.94	1.5	98.14	1.559	10.516	1.67	2.59	1.815

Appendix F

Appendix Table 5. DNA qPCR raw data.

Well	Extraction	Amplicon	Species	Preservation	Ct	Tm (°C)
A1	Proteinase K	B2M	NEG		Undet.	86.1
A2	Proteinase K	B2M	sheep	F1	2.7	77.3
A3	Proteinase K	B2M	deer	FF1	30.64	72.3
A4	TRIzol®	B2M	cow	FF2	32	72
A5	TRIzol®	B2M	sheep	FFPE2	32.67	72.3
A6	Proteinase K	GAPDH	Positive		Undet.	67.6
A7	Proteinase K	GAPDH	sheep	F2	2.29	82.5
A8	Proteinase K	GAPDH	deer	FF2	Undet.	67.6
A9	TRIzol®	GAPDH	cow	FFPE1	Undet.	75
A10	TRIzol®	GAPDH	deer	F1	2.95	83.5
B1	Proteinase K	B2M	Postive		31.13	78.3
B2	Proteinase K	B2M	sheep	F2	2.88	77.6
B3	Proteinase K	B2M	deer	FF2	Undet.	67.6
B4	TRIzol®	B2M	cow	FFPE1	30.91	77.9
B5	TRIzol®	B2M	deer	F1	2.19	78.9
B6	Proteinase K	GAPDH	cow	F1	Undet.	67.6
B7	Proteinase K	GAPDH	sheep	FF1	Undet.	67.6
B8	Proteinase K	GAPDH	deer	FFPE1	Undet.	67.6
B9	TRIzol®	GAPDH	cow	FFPE2	31.22	83.8
B10	TRIzol®	GAPDH	deer	F2	20.08	83.5
C1	Proteinase K	B2M	cow	F1	20.05	78.3
C2	Proteinase K	B2M	sheep	FF1	34.04	73
C3	Proteinase K	B2M	deer	FFPE1	32.52	72.7
C4	TRIzol®	B2M	cow	FFPE2	33.22	78.3
C5	TRIzol®	B2M	deer	F2	25.22	79.6
C6	Proteinase K	GAPDH	cow	F2	Undet.	67.6
C7	Proteinase K	GAPDH	sheep	FF2	Undet.	67.6
C8	Proteinase K	GAPDH	deer	FFPE2	Undet.	67.6
C9	TRIzol®	GAPDH	sheep	F1	21.15	82.8
C10	TRIzol®	GAPDH	deer	FF1	31.45	83.8
D1	Proteinase K	B2M	cow	F2	19.04	78.3
D2	Proteinase K	B2M	sheep	FF2	32.85	73
D3	Proteinase K	B2M	deer	FFPE2	33.12	73
D4	TRIzol®	B2M	sheep	F1	23.06	78.3
D5	TRIzol®	B2M	deer	FF1	31.9	73
D6	Proteinase K	GAPDH	cow	FF1	Undet.	67.6

D7	Proteinase K	GAPDH	sheep	FFPE1	Undet.	67.6
D8	TRIzol®	GAPDH	NEG		28.78	83.2
D9	TRIzol®	GAPDH	sheep	F2	19.68	82.8
D10	TRIzol®	GAPDH	deer	FF2	Undet.	68.9
E1	Proteinase K	B2M	cow	FF1	Undet.	67.6
E2	Proteinase K	B2M	sheep	FFPE1	31.63	72.7
E3	TRIzol®	B2M	NEG		30.15	78.6
E4	TRIzol®	B2M	sheep	F2	23.44	78.3
E5	TRIzol®	B2M	deer	FF2	31	78.6
E6	Proteinase K	GAPDH	cow	FF2	Undet.	67.6
E7	Proteinase K	GAPDH	sheep	FFPE2	Undet.	67.6
E8	TRIzol®	GAPDH	cow	F1	31.67	83.2
E9	TRIzol®	GAPDH	sheep	FF1	32.87	83.8
E10	TRIzol®	GAPDH	deer	FFPE1	33.24	83.5
F1	Proteinase K	B2M	cow	FF2	Undet.	72.7
F2	Proteinase K	B2M	sheep	FFPE2	32.97	72.7
F3	TRIzol®	B2M	cow	F1	2.54	77.9
F4	TRIzol®	B2M	sheep	FF1	31.45	72.7
F5	TRIzol®	B2M	deer	FFPE1	32.79	78.6
F6	Proteinase K	GAPDH	cow	FFPE1	Undet.	67.6
F7	Proteinase K	GAPDH	deer	F1	3.16	83.8
F8	TRIzol®	GAPDH	cow	F2	31.16	83.8
F9	TRIzol®	GAPDH	sheep	FF2	Undet.	67.6
F10	TRIzol®	GAPDH	deer	FFPE2	Undet.	67.6
G1	Proteinase K	B2M	cow	FFPE1	Undet.	67.6
G2	Proteinase K	B2M	deer	F1	3.82	78.9
G3	TRIzol®	B2M	cow	F2	21.96	77.9
G4	TRIzol®	B2M	sheep	FF2	32.28	73
G5	TRIzol®	B2M	deer	FFPE2	32.81	72.3
G6	Proteinase K	GAPDH	cow	FFPE2	Undet.	67.6
G7	Proteinase K	GAPDH	deer	F2	3.83	83.8
G8	TRIzol®	GAPDH	cow	FF1	33.19	83.5
G9	TRIzol®	GAPDH	sheep	FFPE1	Undet.	67.6
H1	Proteinase K	B2M	cow	FFPE2	34.13	72.3
H2	Proteinase K	B2M	deer	F2	3.99	78.9
H3	TRIzol®	B2M	cow	FF1	32.49	78.3
H4	TRIzol®	B2M	sheep	FFPE1	Undet.	67.6
H5	Proteinase K	GAPDH	NEG		Undet.	82.8
H6	Proteinase K	GAPDH	sheep	F1	2.58	82.5
H7	Proteinase K	GAPDH	deer	FF1	Undet.	67.6

H8	TRIzol®	GAPDH	cow	FF2	31.59	83.5
H9	TRIzol®	GAPDH	sheep	FFPE2	33.82	82.8
A1	B2M	PCR	NEG		Undet.	73
A4	GAPDH	PCR	NEG		Undet.	73

Appendix G

Appendix Table 6. RNA RT-qPCR raw data.

Well	Extraction	Amplicon	Species	Preservation	Ct	Tm (°C)
A1	GuSCN	B2M	NEG		Undet.	78
A2	GuSCN	B2M	sheep	Frozen	4.92	77.4
A3	GuSCN	B2M	deer	FF	33.78	78
A4	TRIzol®	B2M	cow	FFPE	31.59	78
A5	TRIzol®	B2M	deer	Frozen	3.3	78.7
A6	GuSCN	GAPDH	cow	FF	Undet.	83.3
A7	GuSCN	GAPDH	sheep	FFPE	26.32	82.4
A8	TRIzol®	GAPDH	cow	Frozen	31.12	83.3
A9	TRIzol®	GAPDH	sheep	FF	32.31	82.7
A10	TRIzol®	GAPDH	deer	FFPE	32.61	83
B1	GuSCN	B2M	cow	Frozen	16.2	77.7
B2	GuSCN	B2M	sheep	FF	34.06	78
B3	GuSCN	B2M	deer	FFPE	33.31	78.4
B4	TRIzol®	B2M	sheep	Frozen	2.81	85.8
B5	TRIzol®	B2M	deer	FF	Undet.	72.4
B6	GuSCN	GAPDH	cow	FF	Undet.	82.7
B7	GuSCN	GAPDH	sheep	FFPE	29.13	82.7
B8	TRIzol®	GAPDH	cow	Frozen	31.08	83.6
B9	TRIzol®	GAPDH	sheep	FF	32.1	83
B10	TRIzol®	GAPDH	deer	FFPE	34.63	83.6
C1	GuSCN	B2M	cow	Frozen	19.19	77.7
C2	GuSCN	B2M	sheep	FF	30.89	72.1
C3	GuSCN	B2M	deer	FFPE	Undet.	78.4
C4	TRIzol®	B2M	sheep	Frozen	3.14	86.1
C5	TRIzol®	B2M	deer	FF	Undet.	72.7
C6	GuSCN	GAPDH	cow	FFPE	Undet.	83.6
C7	GuSCN	GAPDH	deer	Frozen	6.35	83.6
C8	TRIzol®	GAPDH	cow	FF	33.57	83.3
C9	TRIzol®	GAPDH	sheep	FFPE	31.3	83
D1	GuSCN	B2M	cow	FF	Undet.	72.7
D2	GuSCN	B2M	sheep	FFPE	30.26	78.4
D3	TRIzol®	B2M	cow	Frozen	19.42	78
D4	TRIzol®	B2M	sheep	FF	Undet.	78.4
D5	TRIzol®	B2M	deer	FFPE	34.29	78.7
D6	GuSCN	GAPDH	cow	FFPE	Undet.	83
D7	GuSCN	GAPDH	deer	Frozen	4.08	83.6

D8	TRIzol®	GAPDH	cow	FF	Undet.	83.3
D9	TRIzol®	GAPDH	sheep	FFPE	32.88	83.3
E1	GuSCN	B2M	cow	FF	30.71	78.4
E2	GuSCN	B2M	sheep	FFPE	33.44	78.4
E3	TRIzol®	B2M	cow	Frozen	20.97	78
E4	TRIzol®	B2M	sheep	FF	Undet.	78.4
E5	TRIzol®	B2M	deer	FFPE	Undet.	72.7
E6	GuSCN	GAPDH	sheep	Frozen	20.7	82.7
E7	GuSCN	GAPDH	deer	FF	Undet.	83.3
E8	TRIzol®	GAPDH	cow	FFPE	32.86	84.3
E9	TRIzol®	GAPDH	deer	Frozen	3.15	83.6
F1	GuSCN	B2M	cow	FFPE	34.6	78.4
F2	GuSCN	B2M	deer	Frozen	30.45	79.3
F3	TRIzol®	B2M	cow	FF	34.06	78.4
F4	TRIzol®	B2M	sheep	FFPE	33.79	78.4
F5	GuSCN	GAPDH	NEG		31.42	83.6
F6	GuSCN	GAPDH	sheep	Frozen	5.77	82.4
F7	GuSCN	GAPDH	deer	FF	Undet.	82.7
F8	TRIzol®	GAPDH	cow	FFPE	33.95	83.3
F9	TRIzol®	GAPDH	deer	Frozen	3.3	83.6
G1	GuSCN	B2M	cow	FFPE	34.59	78
G2	GuSCN	B2M	deer	Frozen	30.83	79
G3	TRIzol®	B2M	cow	FF	31.8	78
G4	TRIzol®	B2M	sheep	FFPE	Undet.	72.4
G5	GuSCN	GAPDH	cow	Frozen	27.23	83
G6	GuSCN	GAPDH	sheep	FF	Undet.	82.7
G7	GuSCN	GAPDH	deer	FFPE	Undet.	83
G8	TRIzol®	GAPDH	sheep	Frozen	3.11	85.8
G9	TRIzol®	GAPDH	deer	FF	Undet.	83.9
H1	GuSCN	B2M	sheep	Frozen	27.21	77.4
H2	GuSCN	B2M	deer	FF	Undet.	78.4
H3	TRIzol®	B2M	cow	FFPE	33.68	78
H4	TRIzol®	B2M	deer	Frozen	3.48	84.9
H5	GuSCN	GAPDH	cow	Frozen	27.7	83
H6	GuSCN	GAPDH	sheep	FF	33.28	83.6
H7	GuSCN	GAPDH	deer	FFPE	30.74	83.3
H8	TRIzol®	GAPDH	sheep	Frozen	3.09	81.8
H9	TRIzol®	GAPDH	deer	FF	28.05	83.3

Appendix H

Appendix Table 7. qPCR DNA samples sent for Sanger sequencing.

DNA samples		
Sample ID	Extraction	Amplicon
Sheep F1	ProtK	β2M
Deer F1	TRIzol®	GAPDH
Deer FF2	ProtK	β2M
Sheep FF1	TRIzol®	GAPDH
Cow FFPE1	TRIzol®	β2M
Cow FFPE2	TRIzol®	GAPDH

Appendix Table 8. RT-qPCR RNA samples sent for Sanger sequencing.

RNA samples		
Sample ID	Extraction	Amplicon
Sheep F1	GuSCN	GAPDH
Deer F2	GuSCN	β2M
Cow FF2	TRIzol®	β2M
Deer FF2	TRIzol®	GAPDH
Sheep FFPE1	GuSCN	β2M
Cow FFPE1	TRIzol®	GAPDH

Appendix I

select all 100 sequences selected — GenBank | Graphics | Distance tree of results | New MSA Viewer

Description	Scientific Name	Max Score	Total Score	Query Cover	E value	Per. Ident	Acc. Len	Accession
PREDICTED: Odocoileus virginianus texanus glyceraldehyde-3-phosphate dehydrogenase (GAPDH), mRNA	Odocoileus virgi...	305	305	100%	5e-79	100.00%	1292	XM_020878738.1
PREDICTED: Bos indicus x Bos taurus glyceraldehyde-3-phosphate dehydrogenase (GAPDH), mRNA	Bos indicus x B...	300	300	100%	2e-77	99.39%	1289	XM_027541122.1
Syncerus caffer glyceraldehyde 3-phosphate dehydrogenase (GAPDH) mRNA, complete cds	Syncerus caffer	300	300	100%	2e-77	99.39%	1060	MF133531.1
PREDICTED: Bubalus bubalis glyceraldehyde-3-phosphate dehydrogenase (GAPDH), mRNA	Bubalus bubalis	300	300	100%	2e-77	99.39%	1323	XM_006065800.2
PREDICTED: Bos indicus glyceraldehyde-3-phosphate dehydrogenase (GAPDH), mRNA	Bos indicus	300	300	100%	2e-77	99.39%	1289	XM_019960295.1
PREDICTED: Bos mutus glyceraldehyde-3-phosphate dehydrogenase (GAPDH), mRNA	Bos mutus	300	300	100%	2e-77	99.39%	1194	XM_014482068.1
Bos taurus glyceraldehyde-3-phosphate dehydrogenase (GAPDH), mRNA	Bos taurus	300	300	100%	2e-77	99.39%	1279	NM_001034034.2
Bos taurus glyceraldehyde-3-phosphate dehydrogenase, mRNA (cDNA clone MGC:127711 IMAGE:7956315...	Bos taurus	300	300	100%	2e-77	99.39%	1280	BC102589.1
Bos taurus mRNA for similar to glyceraldehyde 3-phosphate dehydrogenase, partial cds, clone: ORCS10594	Bos taurus	300	300	100%	2e-77	99.39%	488	AB098934.1
Bos taurus mRNA for similar to glyceraldehyde 3-phosphate dehydrogenase, partial cds, clone: ORCS10274	Bos taurus	300	300	100%	2e-77	99.39%	556	AB098907.1
Bos grunniens glyceraldehyde-3-phosphate dehydrogenase (gapdh) mRNA, complete cds	Bos grunniens	294	294	100%	1e-75	98.79%	1008	EU195062.1
Bos taurus mRNA for similar to glyceraldehyde 3-phosphate dehydrogenase, partial cds, clone: ORCS11581	Bos taurus	294	294	100%	1e-75	98.80%	610	AB098979.1
PREDICTED: Capra hircus glyceraldehyde-3-phosphate dehydrogenase (GAPDH), mRNA	Capra hircus	289	289	100%	5e-74	98.18%	1306	XM_005680968.3
PREDICTED: Bison bison bison glyceraldehyde-3-phosphate dehydrogenase (GAPDH), mRNA	Bison bison bison	289	289	96%	5e-74	99.37%	1177	XM_010844969.1
PREDICTED: Oryx dammah glyceraldehyde-3-phosphate dehydrogenase (GAPDH), transcript variant X2,...	Oryx dammah	289	289	100%	5e-74	98.18%	1407	XM_040234972.1
PREDICTED: Oryx dammah glyceraldehyde-3-phosphate dehydrogenase (GAPDH), transcript variant X1,...	Oryx dammah	289	289	100%	5e-74	98.18%	1620	XR_005719936.1
PREDICTED: Ovis aries glyceraldehyde-3-phosphate dehydrogenase-like (LOC114110581), mRNA	Ovis aries	283	283	100%	2e-72	97.58%	1270	XM_027961471.1

Appendix Figure 1. NCBI Blast search results for DNA Deer F1 GAPDH forward TRIzol® extracted.

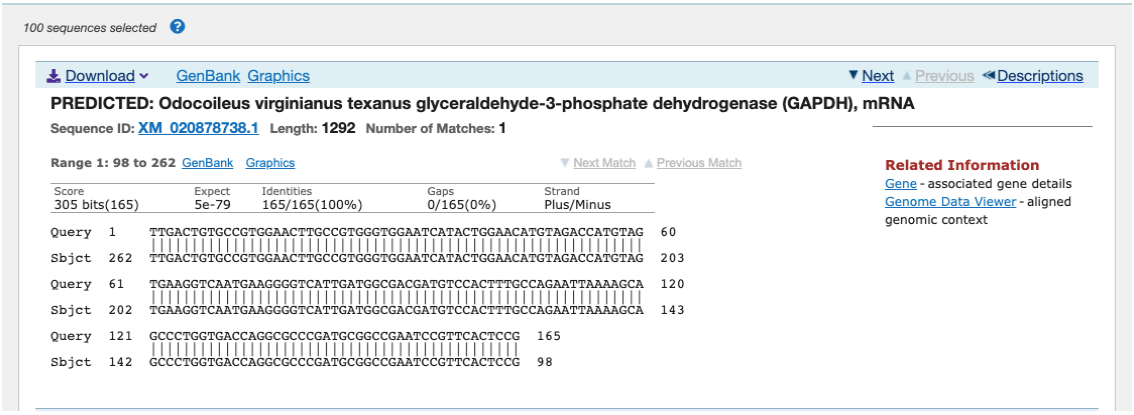

100 sequences selected

Download | GenBank Graphics — Next Previous Descriptions

PREDICTED: Odocoileus virginianus texanus glyceraldehyde-3-phosphate dehydrogenase (GAPDH), mRNA

Sequence ID: XM_020878738.1 Length: 1292 Number of Matches: 1

Range 1: 98 to 262 GenBank Graphics — Next Match Previous Match

Score	Expect	Identities	Gaps	Strand
305 bits(165)	5e-79	165/165(100%)	0/165(0%)	Plus/Minus

```
Query  1    TTGACTGTGCCGTGGAACTTGCCGTGGGTGGAATCATACTGGAACATGTAGACCATGTAG  60
            ||||||||||||||||||||||||||||||||||||||||||||||||||||||||||||
Sbjct  262  TTGACTGTGCCGTGGAACTTGCCGTGGGTGGAATCATACTGGAACATGTAGACCATGTAG  203

Query  61   TGAAGGTCAATGAAGGGGTCATTGATGGCGACGATGTCCACTTTGCCAGAATTAAAAGCA  120
            ||||||||||||||||||||||||||||||||||||||||||||||||||||||||||||
Sbjct  202  TGAAGGTCAATGAAGGGGTCATTGATGGCGACGATGTCCACTTTGCCAGAATTAAAAGCA  143

Query  121  GCCCTGGTGACCAGGCGCCCGATGCGGCCGAATCCGTTCACTCCG  165
            |||||||||||||||||||||||||||||||||||||||||||||
Sbjct  142  GCCCTGGTGACCAGGCGCCCGATGCGGCCGAATCCGTTCACTCCG  98
```

Related Information
Gene - associated gene details
Genome Data Viewer - aligned genomic context

Appendix Figure 2. Sequence alignment for DNA Deer F1 GAPDH forward TRIzol® extracted.

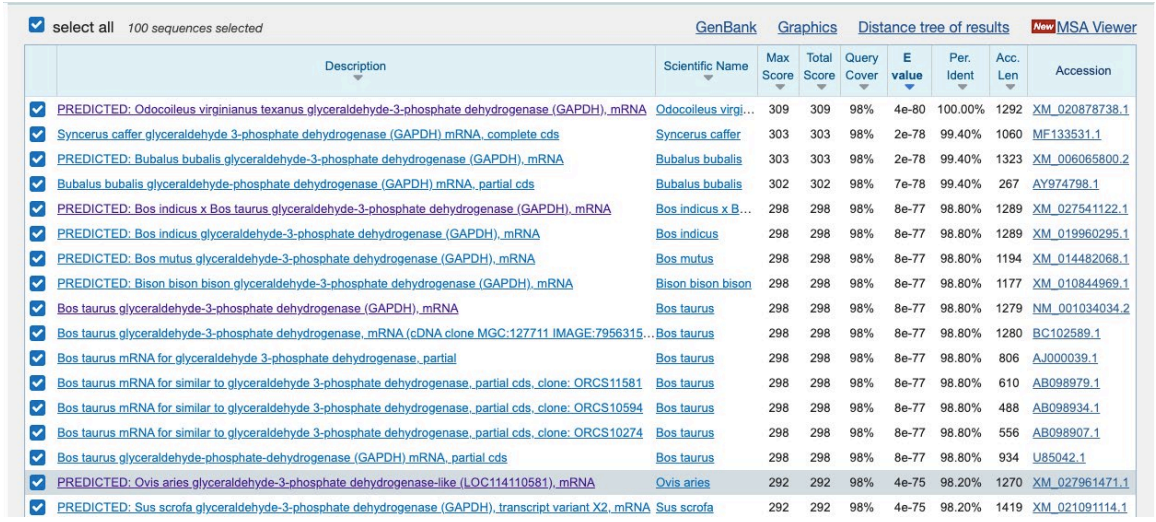

select all 100 sequences selected GenBank Graphics Distance tree of results New MSA Viewer

Description	Scientific Name	Max Score	Total Score	Query Cover	E value	Per. Ident	Acc. Len	Accession
PREDICTED: Odocoileus virginianus texanus glyceraldehyde-3-phosphate dehydrogenase (GAPDH), mRNA	Odocoileus virgi…	309	309	98%	4e-80	100.00%	1292	XM_020878738.1
Syncerus caffer glyceraldehyde 3-phosphate dehydrogenase (GAPDH) mRNA, complete cds	Syncerus caffer	303	303	98%	2e-78	99.40%	1060	MF133531.1
PREDICTED: Bubalus bubalis glyceraldehyde-3-phosphate dehydrogenase (GAPDH), mRNA	Bubalus bubalis	303	303	98%	2e-78	99.40%	1323	XM_006065800.2
Bubalus bubalis glyceraldehyde-phosphate dehydrogenase (GAPDH) mRNA, partial cds	Bubalus bubalis	302	302	98%	7e-78	99.40%	267	AY974798.1
PREDICTED: Bos indicus x Bos taurus glyceraldehyde-3-phosphate dehydrogenase (GAPDH), mRNA	Bos indicus x B…	298	298	98%	8e-77	98.80%	1289	XM_027541122.1
PREDICTED: Bos indicus glyceraldehyde-3-phosphate dehydrogenase (GAPDH), mRNA	Bos indicus	298	298	98%	8e-77	98.80%	1289	XM_019960295.1
PREDICTED: Bos mutus glyceraldehyde-3-phosphate dehydrogenase (GAPDH), mRNA	Bos mutus	298	298	98%	8e-77	98.80%	1194	XM_014482068.1
PREDICTED: Bison bison bison glyceraldehyde-3-phosphate dehydrogenase (GAPDH), mRNA	Bison bison bison	298	298	98%	8e-77	98.80%	1177	XM_010844969.1
Bos taurus glyceraldehyde-3-phosphate dehydrogenase (GAPDH), mRNA	Bos taurus	298	298	98%	8e-77	98.80%	1279	NM_001034034.2
Bos taurus glyceraldehyde-3-phosphate dehydrogenase, mRNA (cDNA clone MGC:127711 IMAGE:7956315…	Bos taurus	298	298	98%	8e-77	98.80%	1280	BC102589.1
Bos taurus mRNA for glyceraldehyde 3-phosphate dehydrogenase, partial	Bos taurus	298	298	98%	8e-77	98.80%	806	AJ000039.1
Bos taurus mRNA for similar to glyceraldehyde 3-phosphate dehydrogenase, partial cds, clone: ORCS11581	Bos taurus	298	298	98%	8e-77	98.80%	610	AB098979.1
Bos taurus mRNA for similar to glyceraldehyde 3-phosphate dehydrogenase, partial cds, clone: ORCS10594	Bos taurus	298	298	98%	8e-77	98.80%	488	AB098934.1
Bos taurus mRNA for similar to glyceraldehyde 3-phosphate dehydrogenase, partial cds, clone: ORCS10274	Bos taurus	298	298	98%	8e-77	98.80%	556	AB098907.1
Bos taurus glyceraldehyde-phosphate-dehydrogenase (GAPDH) mRNA, partial cds	Bos taurus	298	298	98%	8e-77	98.80%	934	U85042.1
PREDICTED: Ovis aries glyceraldehyde-3-phosphate dehydrogenase-like (LOC114110581), mRNA	Ovis aries	292	292	98%	4e-75	98.20%	1270	XM_027961471.1
PREDICTED: Sus scrofa glyceraldehyde-3-phosphate dehydrogenase (GAPDH), transcript variant X2, mRNA	Sus scrofa	292	292	98%	4e-75	98.20%	1419	XM_021091114.1

Appendix Figure 3. NCBI Blast search results for DNA Deer F1 GAPDH reverse TRIzol® extracted.

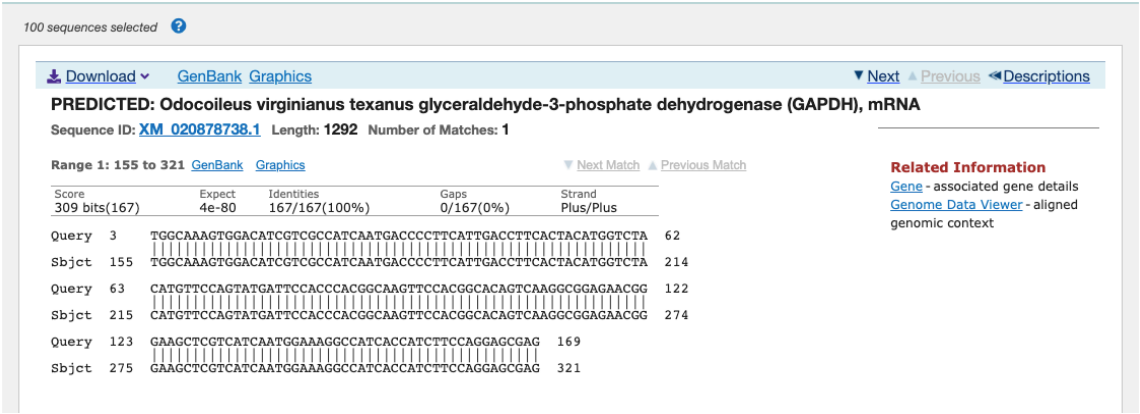

100 sequences selected

Download GenBank Graphics Next Previous Descriptions

PREDICTED: Odocoileus virginianus texanus glyceraldehyde-3-phosphate dehydrogenase (GAPDH), mRNA

Sequence ID: XM_020878738.1 Length: 1292 Number of Matches: 1

Range 1: 155 to 321 GenBank Graphics Next Match Previous Match

Score	Expect	Identities	Gaps	Strand
309 bits(167)	4e-80	167/167(100%)	0/167(0%)	Plus/Plus

```
Query  3    TGGCAAAGTGGACATCGTCGCCATCAATGACCCCTTCATTGACCTTCACTACATGGTCTA  62
            ||||||||||||||||||||||||||||||||||||||||||||||||||||||||||||
Sbjct  155  TGGCAAAGTGGACATCGTCGCCATCAATGACCCCTTCATTGACCTTCACTACATGGTCTA  214

Query  63   CATGTTCCAGTATGATTCCACCCACGGCAAGTTCCACGGCACAGTCAAGGCGGAGAACGG  122
            ||||||||||||||||||||||||||||||||||||||||||||||||||||||||||||
Sbjct  215  CATGTTCCAGTATGATTCCACCCACGGCAAGTTCCACGGCACAGTCAAGGCGGAGAACGG  274

Query  123  GAAGCTCGTCATCAATGGAAAGGCCATCACCATCTTCCAGGAGCGAG  169
            |||||||||||||||||||||||||||||||||||||||||||||||
Sbjct  275  GAAGCTCGTCATCAATGGAAAGGCCATCACCATCTTCCAGGAGCGAG  321
```

Related Information
Gene - associated gene details
Genome Data Viewer - aligned genomic context

Appendix Figure 4. Sequence alignment for DNA Deer F1 GAPDH reverse TRIzol® extracted.

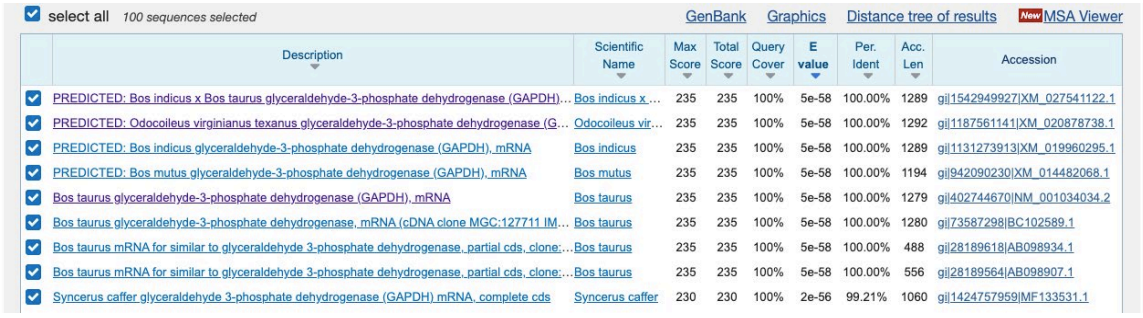

select all 100 sequences selected GenBank Graphics Distance tree of results New MSA Viewer

Description	Scientific Name	Max Score	Total Score	Query Cover	E value	Per. Ident	Acc. Len	Accession
PREDICTED: Bos indicus x Bos taurus glyceraldehyde-3-phosphate dehydrogenase (GAPDH)…	Bos indicus x …	235	235	100%	5e-58	100.00%	1289	gi|1542949927|XM_027541122.1
PREDICTED: Odocoileus virginianus texanus glyceraldehyde-3-phosphate dehydrogenase (G…	Odocoileus vir…	235	235	100%	5e-58	100.00%	1292	gi|1187561141|XM_020878738.1
PREDICTED: Bos indicus glyceraldehyde-3-phosphate dehydrogenase (GAPDH), mRNA	Bos indicus	235	235	100%	5e-58	100.00%	1289	gi|1131273913|XM_019960295.1
PREDICTED: Bos mutus glyceraldehyde-3-phosphate dehydrogenase (GAPDH), mRNA	Bos mutus	235	235	100%	5e-58	100.00%	1194	gi|942090230|XM_014482068.1
Bos taurus glyceraldehyde-3-phosphate dehydrogenase (GAPDH), mRNA	Bos taurus	235	235	100%	5e-58	100.00%	1279	gi|402744670|NM_001034034.2
Bos taurus glyceraldehyde-3-phosphate dehydrogenase, mRNA (cDNA clone MGC:127711 IM…	Bos taurus	235	235	100%	5e-58	100.00%	1280	gi|73587298|BC102589.1
Bos taurus mRNA for similar to glyceraldehyde 3-phosphate dehydrogenase, partial cds, clone:…	Bos taurus	235	235	100%	5e-58	100.00%	488	gi|28189618|AB098934.1
Bos taurus mRNA for similar to glyceraldehyde 3-phosphate dehydrogenase, partial cds, clone:…	Bos taurus	235	235	100%	5e-58	100.00%	556	gi|28189564|AB098907.1
Syncerus caffer glyceraldehyde 3-phosphate dehydrogenase (GAPDH) mRNA, complete cds	Syncerus caffer	230	230	100%	2e-56	99.21%	1060	gi|1424757959|MF133531.1

Appendix Figure 5. NCBI Blast search results for DNA Cow FFPE2 GAPDH forward TRIzol® extracted.

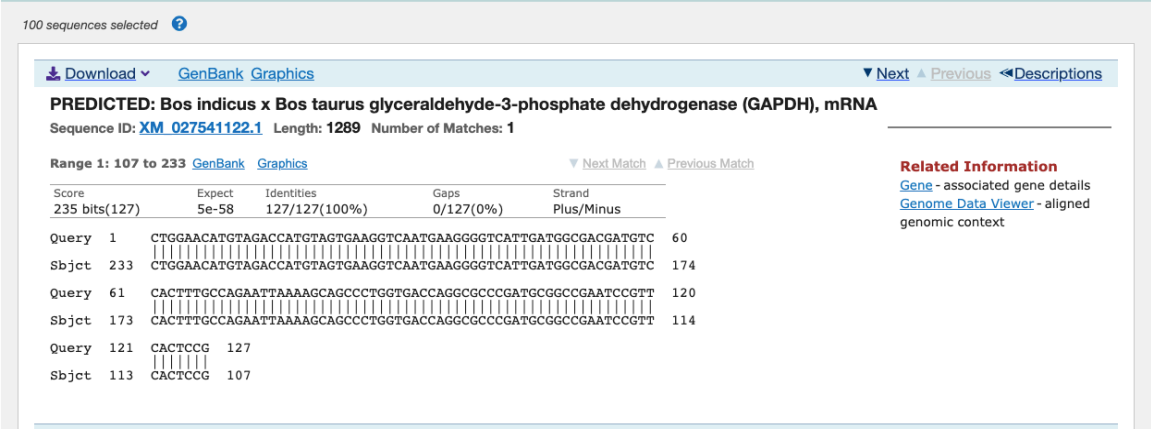

Appendix Figure 6. Sequence alignment for DNA Cow FFPE2 GAPDH forward TRIzol® extracted.

Description	Scientific Name	Max Score	Total Score	Query Cover	E value	Per. Ident	Acc. Len	Accession
PREDICTED: Odocoileus virginianus texanus glyceraldehyde-3-phosphate dehydrogenase (GAPDH), mRNA	Odocoileus virgi...	305	305	100%	5e-79	100.00%	1292	XM_020878738.1
PREDICTED: Bos indicus x Bos taurus glyceraldehyde-3-phosphate dehydrogenase (GAPDH), mRNA	Bos indicus x B...	300	300	100%	2e-77	99.39%	1289	XM_027541122.1
Syncerus caffer glyceraldehyde 3-phosphate dehydrogenase (GAPDH) mRNA, complete cds	Syncerus caffer	300	300	100%	2e-77	99.39%	1060	MF133531.1
PREDICTED: Bubalus bubalis glyceraldehyde-3-phosphate dehydrogenase (GAPDH), mRNA	Bubalus bubalis	300	300	100%	2e-77	99.39%	1323	XM_006065800.2
PREDICTED: Bos indicus glyceraldehyde-3-phosphate dehydrogenase (GAPDH), mRNA	Bos indicus	300	300	100%	2e-77	99.39%	1289	XM_019960295.1
PREDICTED: Bos mutus glyceraldehyde-3-phosphate dehydrogenase (GAPDH), mRNA	Bos mutus	300	300	100%	2e-77	99.39%	1194	XM_014482068.1
Bos taurus glyceraldehyde-3-phosphate dehydrogenase (GAPDH), mRNA	Bos taurus	300	300	100%	2e-77	99.39%	1279	NM_001034034.2
Bos taurus glyceraldehyde-3-phosphate dehydrogenase, mRNA (cDNA clone MGC:127711 IMAGE:7956315...	Bos taurus	300	300	100%	2e-77	99.39%	1280	BC102589.1
Bos taurus mRNA for similar to glyceraldehyde 3-phosphate dehydrogenase, partial cds, clone: ORCS10594	Bos taurus	300	300	100%	2e-77	99.39%	488	AB098934.1
Bos taurus mRNA for similar to glyceraldehyde 3-phosphate dehydrogenase, partial cds, clone: ORCS10274	Bos taurus	300	300	100%	2e-77	99.39%	556	AB098907.1
Bos grunniens glyceraldehyde-3-phosphate dehydrogenase (gapdh) mRNA, complete cds	Bos grunniens	294	294	100%	1e-75	98.79%	1008	EU195062.1
Bos taurus mRNA for similar to glyceraldehyde 3-phosphate dehydrogenase, partial cds, clone: ORCS11581	Bos taurus	294	294	100%	1e-75	98.80%	610	AB098979.1
PREDICTED: Capra hircus glyceraldehyde-3-phosphate dehydrogenase (GAPDH), mRNA	Capra hircus	289	289	100%	5e-74	98.18%	1306	XM_005680968.3
PREDICTED: Bison bison bison glyceraldehyde-3-phosphate dehydrogenase (GAPDH), mRNA	Bison bison bison	289	289	96%	5e-74	99.37%	1177	XM_010844969.1
PREDICTED: Oryx dammah glyceraldehyde-3-phosphate dehydrogenase (GAPDH), transcript variant X2,...	Oryx dammah	289	289	100%	5e-74	98.18%	1407	XM_040234972.1
PREDICTED: Oryx dammah glyceraldehyde-3-phosphate dehydrogenase (GAPDH), transcript variant X1,...	Oryx dammah	289	289	100%	5e-74	98.18%	1620	XR_005719936.1
PREDICTED: Ovis aries glyceraldehyde-3-phosphate dehydrogenase-like (LOC114110581), mRNA	Ovis aries	283	283	100%	2e-72	97.58%	1270	XM_027961471.1

Appendix Figure 7. NCBI Blast search results for RNA Deer FF2 GAPDH forward TRIzol® extracted.

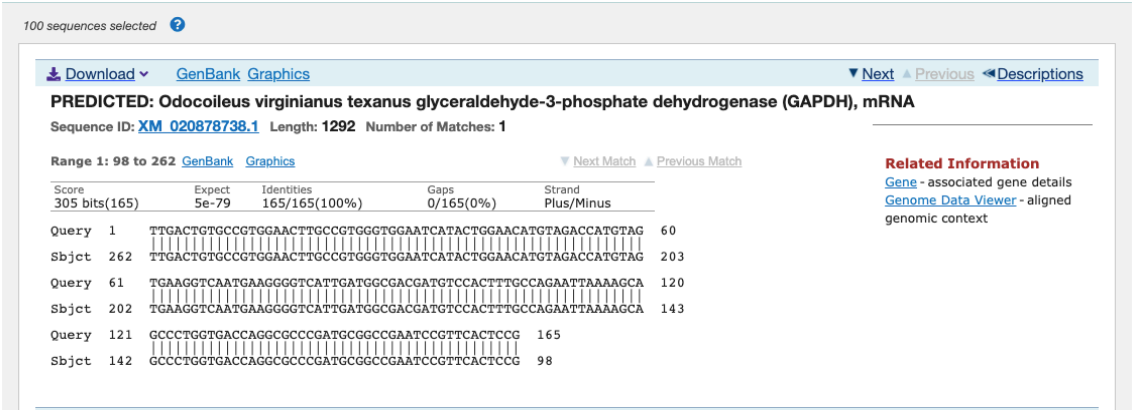

Appendix Figure 8. Sequence alignment for RNA Deer FF2 GAPDH forward TRIzol® extracted.

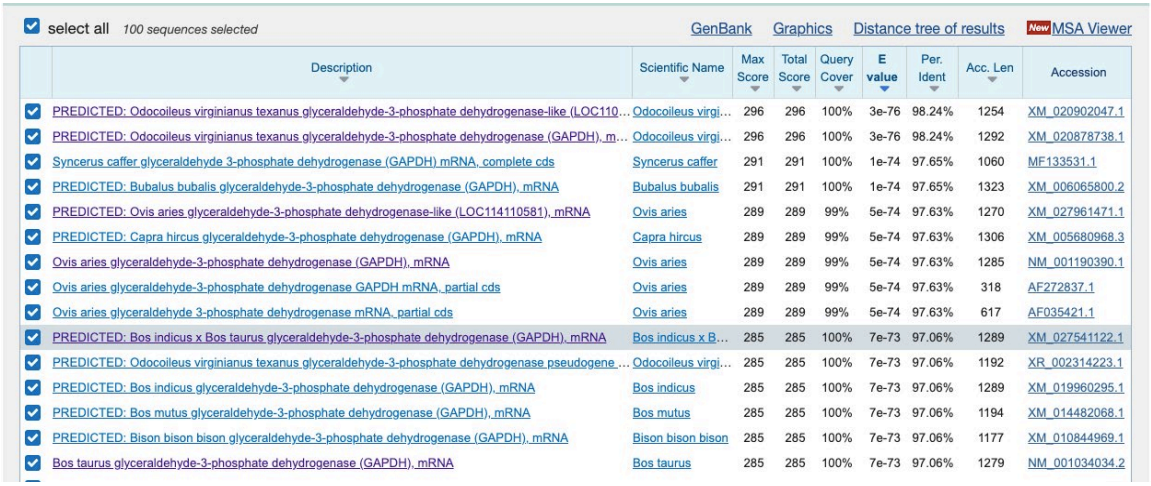

Description	Scientific Name	Max Score	Total Score	Query Cover	E value	Per. Ident	Acc. Len	Accession
PREDICTED: Odocoileus virginianus texanus glyceraldehyde-3-phosphate dehydrogenase-like (LOC110…	Odocoileus virgi…	296	296	100%	3e-76	98.24%	1254	XM_020902047.1
PREDICTED: Odocoileus virginianus texanus glyceraldehyde-3-phosphate dehydrogenase (GAPDH), m…	Odocoileus virgi…	296	296	100%	3e-76	98.24%	1292	XM_020878738.1
Syncerus caffer glyceraldehyde 3-phosphate dehydrogenase (GAPDH) mRNA, complete cds	Syncerus caffer	291	291	100%	1e-74	97.65%	1060	MF133531.1
PREDICTED: Bubalus bubalis glyceraldehyde-3-phosphate dehydrogenase (GAPDH), mRNA	Bubalus bubalis	291	291	100%	1e-74	97.65%	1323	XM_006065800.2
PREDICTED: Ovis aries glyceraldehyde-3-phosphate dehydrogenase-like (LOC114110581), mRNA	Ovis aries	289	289	99%	5e-74	97.63%	1270	XM_027961471.1
PREDICTED: Capra hircus glyceraldehyde-3-phosphate dehydrogenase (GAPDH), mRNA	Capra hircus	289	289	99%	5e-74	97.63%	1306	XM_005680968.3
Ovis aries glyceraldehyde-3-phosphate dehydrogenase (GAPDH), mRNA	Ovis aries	289	289	99%	5e-74	97.63%	1285	NM_001190390.1
Ovis aries glyceraldehyde-3-phosphate dehydrogenase GAPDH mRNA, partial cds	Ovis aries	289	289	99%	5e-74	97.63%	318	AF272837.1
Ovis aries glyceraldehyde 3-phosphate dehydrogenase mRNA, partial cds	Ovis aries	289	289	99%	5e-74	97.63%	617	AF035421.1
PREDICTED: Bos indicus x Bos taurus glyceraldehyde-3-phosphate dehydrogenase (GAPDH), mRNA	Bos indicus x B…	285	285	100%	7e-73	97.06%	1289	XM_027541122.1
PREDICTED: Odocoileus virginianus texanus glyceraldehyde-3-phosphate dehydrogenase pseudogene …	Odocoileus virgi…	285	285	100%	7e-73	97.06%	1192	XR_002314223.1
PREDICTED: Bos indicus glyceraldehyde-3-phosphate dehydrogenase (GAPDH), mRNA	Bos indicus	285	285	100%	7e-73	97.06%	1289	XM_019960295.1
PREDICTED: Bos mutus glyceraldehyde-3-phosphate dehydrogenase (GAPDH), mRNA	Bos mutus	285	285	100%	7e-73	97.06%	1194	XM_014482068.1
PREDICTED: Bison bison bison glyceraldehyde-3-phosphate dehydrogenase (GAPDH), mRNA	Bison bison bison	285	285	100%	7e-73	97.06%	1177	XM_010844969.1
Bos taurus glyceraldehyde-3-phosphate dehydrogenase (GAPDH), mRNA	Bos taurus	285	285	100%	7e-73	97.06%	1279	NM_001034034.2

Appendix Figure 9. NCBI Blast search results for RNA Deer FF2 GAPDH reverse TRIzol® extracted.

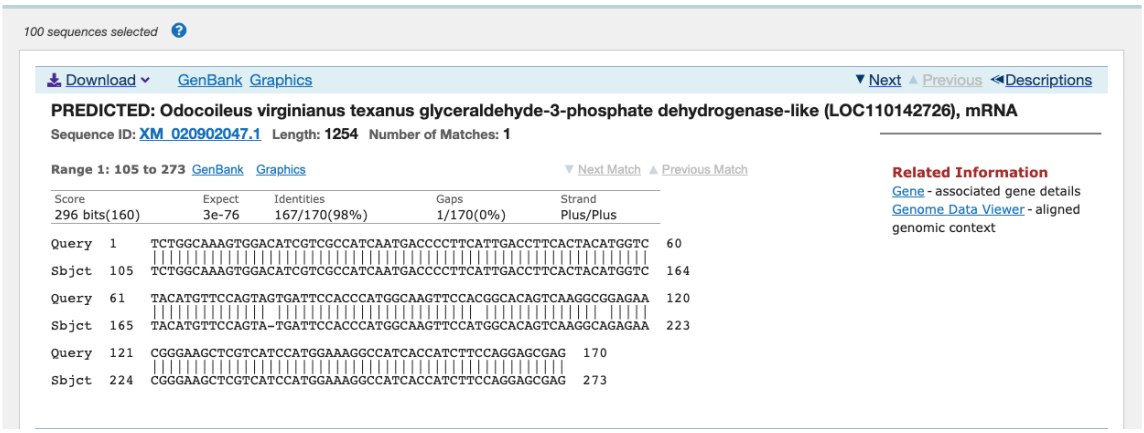

Appendix Figure 10. Sequence alignment for RNA Deer FF2 GAPDH reverse TRIzol® extracted.

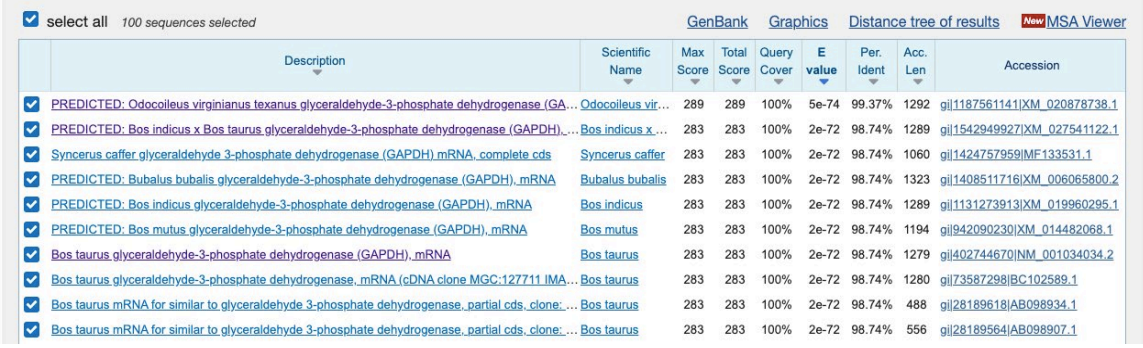

Appendix Figure 11. NCBI Blast search results for RNA Cow FFPE1 GAPDH forward TRIzol® extracted.

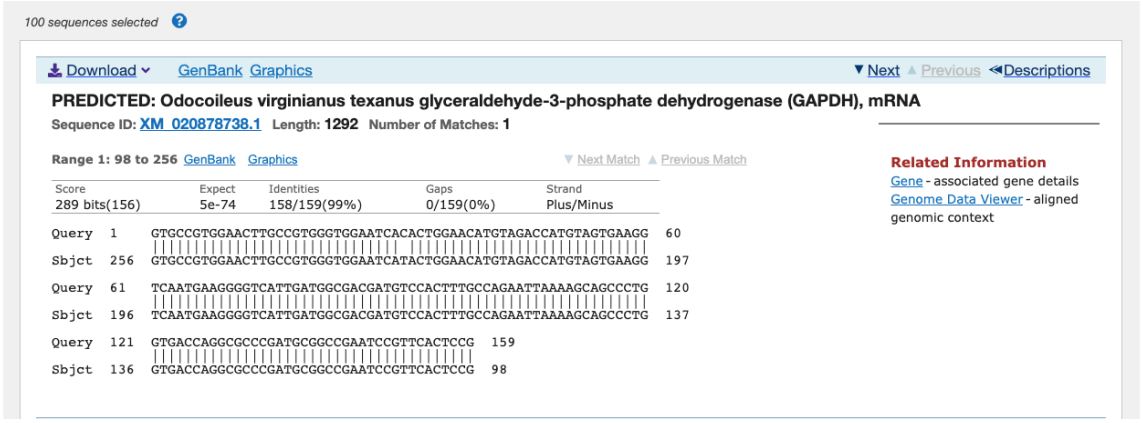

Appendix Figure 12. Sequence alignment 1 for RNA Cow FFPE1 GAPDH forward TRIzol® extracted.

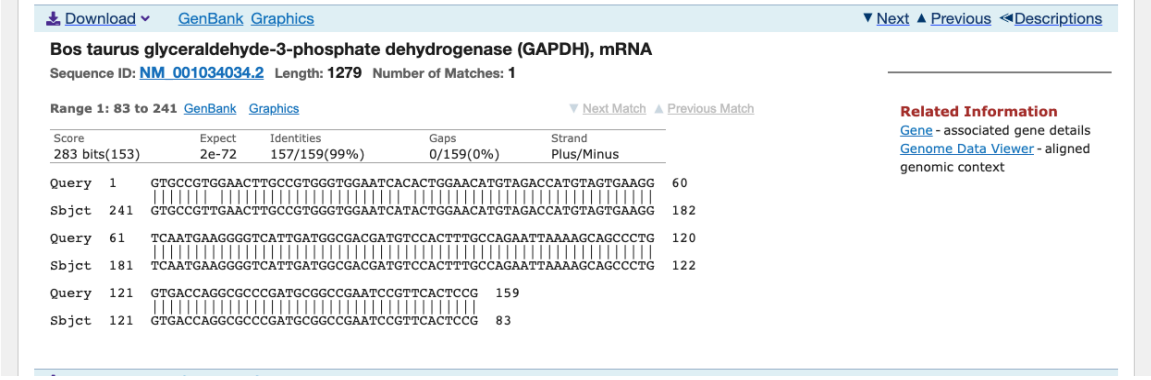

Appendix Figure 13. Sequence alignment 2 for RNA Cow FFPE1 GAPDH forward TRIzol® extracted.

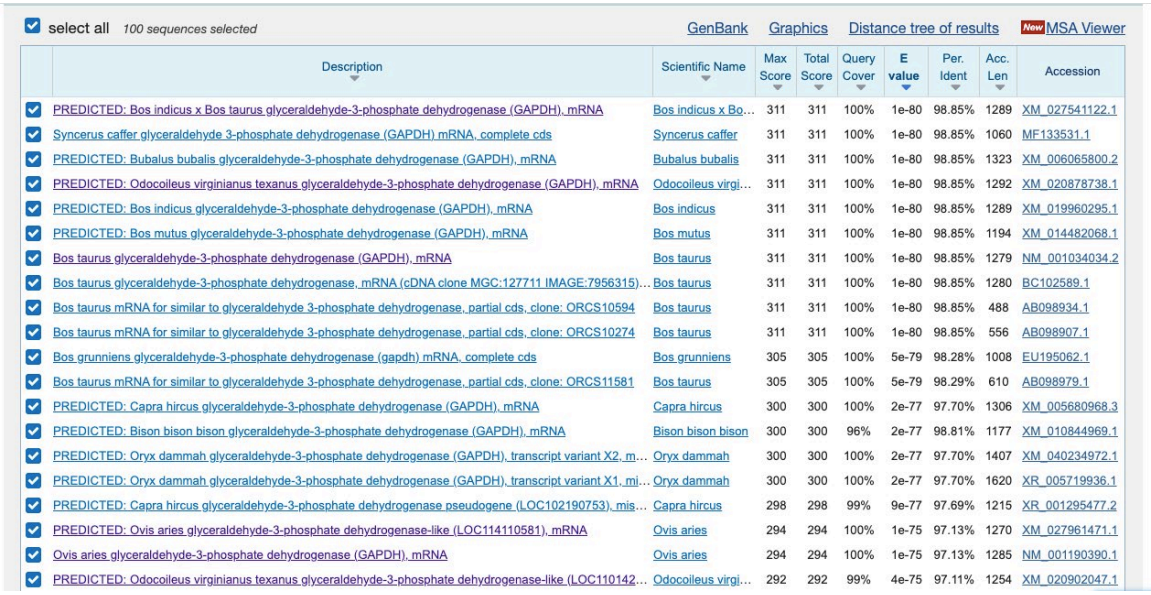

Description	Scientific Name	Max Score	Total Score	Query Cover	E value	Per. Ident	Acc. Len	Accession
PREDICTED: Bos indicus x Bos taurus glyceraldehyde-3-phosphate dehydrogenase (GAPDH), mRNA	Bos indicus x Bo…	311	311	100%	1e-80	98.85%	1289	XM_027541122.1
Syncerus caffer glyceraldehyde 3-phosphate dehydrogenase (GAPDH) mRNA, complete cds	Syncerus caffer	311	311	100%	1e-80	98.85%	1060	MF133531.1
PREDICTED: Bubalus bubalis glyceraldehyde-3-phosphate dehydrogenase (GAPDH), mRNA	Bubalus bubalis	311	311	100%	1e-80	98.85%	1323	XM_006065800.2
PREDICTED: Odocoileus virginianus texanus glyceraldehyde-3-phosphate dehydrogenase (GAPDH), mRNA	Odocoileus virgi…	311	311	100%	1e-80	98.85%	1292	XM_020878738.1
PREDICTED: Bos indicus glyceraldehyde-3-phosphate dehydrogenase (GAPDH), mRNA	Bos indicus	311	311	100%	1e-80	98.85%	1289	XM_019960295.1
PREDICTED: Bos mutus glyceraldehyde-3-phosphate dehydrogenase (GAPDH), mRNA	Bos mutus	311	311	100%	1e-80	98.85%	1194	XM_014482068.1
Bos taurus glyceraldehyde-3-phosphate dehydrogenase (GAPDH), mRNA	Bos taurus	311	311	100%	1e-80	98.85%	1279	NM_001034034.2
Bos taurus glyceraldehyde-3-phosphate dehydrogenase, mRNA (cDNA clone MGC:127711 IMAGE:7956315)…	Bos taurus	311	311	100%	1e-80	98.85%	1280	BC102589.1
Bos taurus mRNA for similar to glyceraldehyde 3-phosphate dehydrogenase, partial cds, clone: ORCS10594	Bos taurus	311	311	100%	1e-80	98.85%	488	AB098934.1
Bos taurus mRNA for similar to glyceraldehyde 3-phosphate dehydrogenase, partial cds, clone: ORCS10274	Bos taurus	311	311	100%	1e-80	98.85%	556	AB098907.1
Bos grunniens glyceraldehyde-3-phosphate dehydrogenase (gapdh) mRNA, complete cds	Bos grunniens	305	305	100%	5e-79	98.28%	1008	EU195062.1
Bos taurus mRNA for similar to glyceraldehyde 3-phosphate dehydrogenase, partial cds, clone: ORCS11581	Bos taurus	305	305	100%	5e-79	98.29%	610	AB098979.1
PREDICTED: Capra hircus glyceraldehyde-3-phosphate dehydrogenase (GAPDH), mRNA	Capra hircus	300	300	100%	2e-77	97.70%	1306	XM_005680968.3
PREDICTED: Bison bison bison glyceraldehyde-3-phosphate dehydrogenase (GAPDH), mRNA	Bison bison bison	300	300	96%	2e-77	98.81%	1177	XM_010844969.1
PREDICTED: Oryx dammah glyceraldehyde-3-phosphate dehydrogenase (GAPDH), transcript variant X2, m…	Oryx dammah	300	300	100%	2e-77	97.70%	1407	XM_040234972.1
PREDICTED: Oryx dammah glyceraldehyde-3-phosphate dehydrogenase (GAPDH), transcript variant X1, mi…	Oryx dammah	300	300	100%	2e-77	97.70%	1620	XR_005719936.1
PREDICTED: Capra hircus glyceraldehyde-3-phosphate dehydrogenase pseudogene (LOC102190753), mis…	Capra hircus	298	298	99%	9e-77	97.69%	1215	XR_001295477.2
PREDICTED: Ovis aries glyceraldehyde-3-phosphate dehydrogenase-like (LOC114110581), mRNA	Ovis aries	294	294	100%	1e-75	97.13%	1270	XM_027961471.1
Ovis aries glyceraldehyde-3-phosphate dehydrogenase (GAPDH), mRNA	Ovis aries	294	294	100%	1e-75	97.13%	1285	NM_001190390.1
PREDICTED: Odocoileus virginianus texanus glyceraldehyde-3-phosphate dehydrogenase-like (LOC110142…	Odocoileus virgi…	292	292	99%	4e-75	97.11%	1254	XM_020902047.1

Appendix Figure 14. NCBI Blast search results for RNA Sheep F1 GAPDH forward GuSCN extracted.

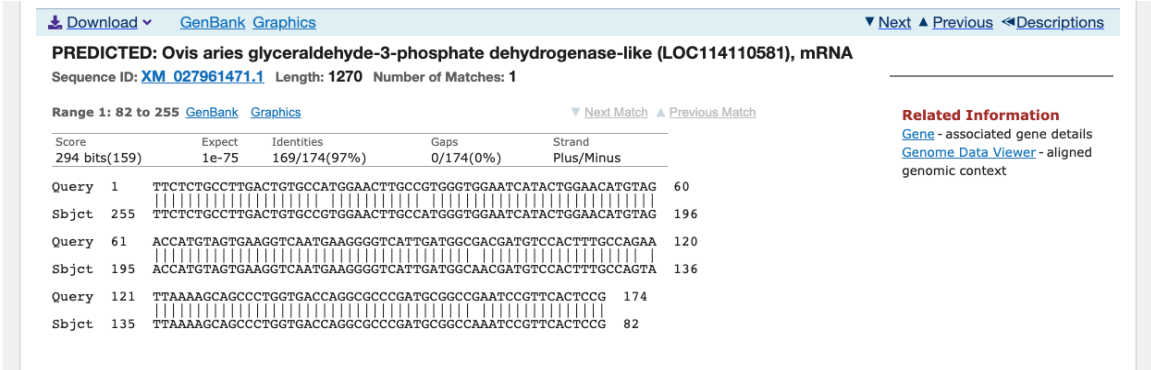

Appendix Figure 15. Sequence alignment 2 for RNA Sheep F1 GAPDH forward GuSCN extracted.

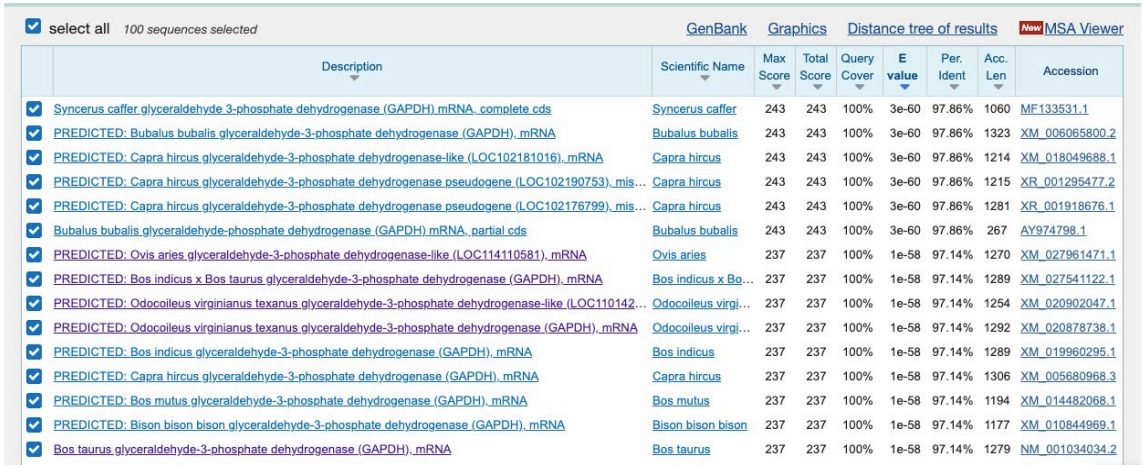

select all 100 sequences selected GenBank Graphics Distance tree of results New MSA Viewer

Description	Scientific Name	Max Score	Total Score	Query Cover	E value	Per. Ident	Acc. Len	Accession
Syncerus caffer glyceraldehyde 3-phosphate dehydrogenase (GAPDH) mRNA, complete cds	Syncerus caffer	243	243	100%	3e-60	97.86%	1060	MF133531.1
PREDICTED: Bubalus bubalis glyceraldehyde-3-phosphate dehydrogenase (GAPDH), mRNA	Bubalus bubalis	243	243	100%	3e-60	97.86%	1323	XM_006065800.2
PREDICTED: Capra hircus glyceraldehyde-3-phosphate dehydrogenase-like (LOC102181016), mRNA	Capra hircus	243	243	100%	3e-60	97.86%	1214	XM_018049688.1
PREDICTED: Capra hircus glyceraldehyde-3-phosphate dehydrogenase pseudogene (LOC102190753), mis...	Capra hircus	243	243	100%	3e-60	97.86%	1215	XR_001295477.2
PREDICTED: Capra hircus glyceraldehyde-3-phosphate dehydrogenase pseudogene (LOC102176799), mis...	Capra hircus	243	243	100%	3e-60	97.86%	1281	XR_001918676.1
Bubalus bubalis glyceraldehyde-phosphate dehydrogenase (GAPDH) mRNA, partial cds	Bubalus bubalis	243	243	100%	3e-60	97.86%	267	AY974798.1
PREDICTED: Ovis aries glyceraldehyde-3-phosphate dehydrogenase-like (LOC114110581), mRNA	Ovis aries	237	237	100%	1e-58	97.14%	1270	XM_027961471.1
PREDICTED: Bos indicus x Bos taurus glyceraldehyde-3-phosphate dehydrogenase (GAPDH), mRNA	Bos indicus x Bo...	237	237	100%	1e-58	97.14%	1289	XM_027541122.1
PREDICTED: Odocoileus virginianus texanus glyceraldehyde-3-phosphate dehydrogenase-like (LOC110142...	Odocoileus virgi...	237	237	100%	1e-58	97.14%	1254	XM_020902047.1
PREDICTED: Odocoileus virginianus texanus glyceraldehyde-3-phosphate dehydrogenase (GAPDH), mRNA	Odocoileus virgi...	237	237	100%	1e-58	97.14%	1292	XM_020878738.1
PREDICTED: Bos indicus glyceraldehyde-3-phosphate dehydrogenase (GAPDH), mRNA	Bos indicus	237	237	100%	1e-58	97.14%	1289	XM_019960295.1
PREDICTED: Capra hircus glyceraldehyde-3-phosphate dehydrogenase (GAPDH), mRNA	Capra hircus	237	237	100%	1e-58	97.14%	1306	XM_005680968.3
PREDICTED: Bos mutus glyceraldehyde-3-phosphate dehydrogenase (GAPDH), mRNA	Bos mutus	237	237	100%	1e-58	97.14%	1194	XM_014482068.1
PREDICTED: Bison bison bison glyceraldehyde-3-phosphate dehydrogenase (GAPDH), mRNA	Bison bison bison	237	237	100%	1e-58	97.14%	1177	XM_010844969.1
Bos taurus glyceraldehyde-3-phosphate dehydrogenase (GAPDH), mRNA	Bos taurus	237	237	100%	1e-58	97.14%	1279	NM_001034034.2

Appendix Figure 16. NCBI Blast search results for RNA Sheep F1 GAPDH reverse GuSCN extracted.

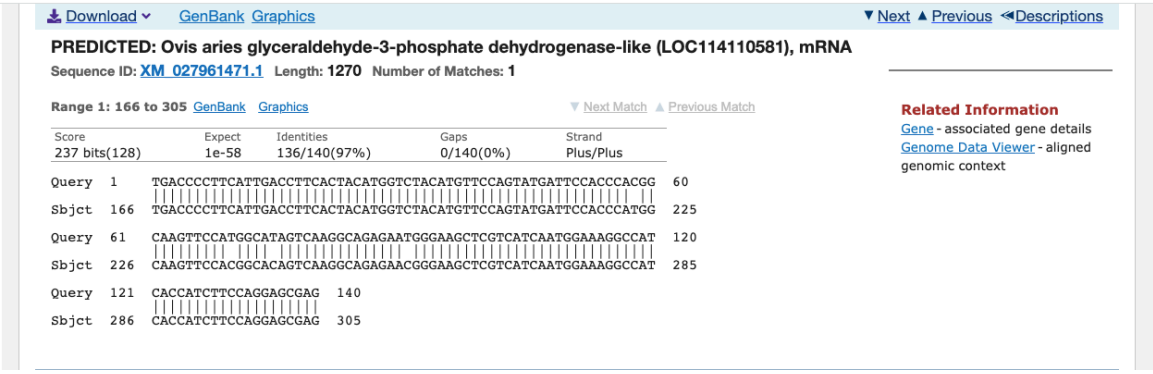

Download GenBank Graphics ▼Next ▲Previous ◀Descriptions

PREDICTED: Ovis aries glyceraldehyde-3-phosphate dehydrogenase-like (LOC114110581), mRNA

Sequence ID: XM_027961471.1 Length: 1270 Number of Matches: 1

Range 1: 166 to 305 GenBank Graphics ▼Next Match ▲Previous Match

Score	Expect	Identities	Gaps	Strand
237 bits(128)	1e-58	136/140(97%)	0/140(0%)	Plus/Plus

```
Query  1    TGACCCCTTCATTGACCTTCACTACATGGTCTACATGTTCCAGTATGATTCCACCCACGG  60
            ||||||||||||||||||||||||||||||||||||||||||||||||||||||||||||
Sbjct  166  TGACCCCTTCATTGACCTTCACTACATGGTCTACATGTTCCAGTATGATTCCACCCATGG  225

Query  61   CAAGTTCCATGGCATAGTCAAGGCAGAGAATGGGAAGCTCGTCATCAATGGAAAGGCCAT  120
            |||||||||  |||| ||||||||||||||  ||||||||||||||||||||||||||||
Sbjct  226  CAAGTTCCACGGCACAGTCAAGGCAGAGAACGGGAAGCTCGTCATCAATGGAAAGGCCAT  285

Query  121  CACCATCTTCCAGGAGCGAG  140
            ||||||||||||||||||||
Sbjct  286  CACCATCTTCCAGGAGCGAG  305
```

Related Information

Gene - associated gene details

Genome Data Viewer - aligned genomic context

Appendix Figure 17. Sequence alignment 2 for RNA Sheep F1 GAPDH reverse GuSCN extracted.